Summer 2011

Use Of Cuencas hydrological model in simulating the effects of land use change on the 2008 flooding event in the Turkey River Watershed

Maria Fernanda Perez Gonzalez
University of Iowa

Follow this and additional works at: https://ir.uiowa.edu/etd
Part of the Civil and Environmental Engineering Commons

USE OF CUENCAS HYDROLOGICAL MODEL IN SIMULATING THE EFFECTS OF LAND USE CHANGE ON THE 2008 FLOODING EVENT IN THE TURKEY RIVER WATERSHED

by

María Fernanda Pérez González

A thesis submitted in partial fulfillment
of the requirements for the
Master of Science degree in
Civil and Environmental Engineering
in the Graduate College of
The University of Iowa

July 2011

Thesis Supervisors: Professor Larry J. Weber
Assistant Research Engineer Ricardo Mantilla

Graduate College
The University of Iowa
Iowa City, Iowa

CERTIFICATE OF APPROVAL

____

MASTER'S THESIS

____

This is to certify that the Master's thesis of

María Fernanda Pérez González

has been approved by the Examining Committee
for the thesis requirement for the Master of Science
degree in Civil and Environmental Engineering at the July 2011 graduation.

Thesis Committee: ___________________________________
Larry J. Weber, Thesis Supervisor

____
Ricardo Mantilla, Thesis Supervisor

____
Witold F. Krajewski

Para Mark y Emma- mis grandes amores

ACKNOWLEDGMENTS

I would like to thank Dr. Larry Weber for inspiring me to go back to school and for all his guidance during these two years. I also want to thank Dr. Ricardo Mantilla for all his time and for sharing with me his passion for hydrological modeling. I specially want to thank Luciana Cunha, for providing so much technical support throughout this thesis. I want to thank my committee members, for their valuable inputs and time. This work was possible thanks to the Iowa Flood Center support.

I want to thank my husband Mark, for being a loving and supporting husband, and for encouraging me when I most need it. I am deeply thankful to my parents, for taking care of Emma while I completed this thesis. I want to thank my friend Miryam, for letting me work from her office. But most important, thanks to God, for giving me a life full of wonderful opportunities.

ABSTRACT

East Iowa experienced large flooding during June of 2008. This study used Cuencas hydrological model to simulate the discharges of June 2008 at Eldorado and Elkader, in the Turkey River Watershed, in North East Iowa. The results of this study were used to test the performance of Cuencas modeling this flood event and to explore the role of land cover change in the floods of 2008 at Elkader, Iowa.

Cuencas was found to be a suitable tool to predict this event and it required relatively low resources. The total time to run each simulation was around two hours which is reasonable for such large watershed (900 mi^2), but a computer cluster was needed to run these simulations.

The results from this study suggest that the role of land cover change from pre-settlement to current conditions was significant when using the rainfall conditions of 2008. The discharges simulated at Elkader, Iowa were almost twice as large when using the 2001 land cover, than when using the land cover found during 1832-1859, recorded during the General Land Office (GLO) survey. These results need to be taken only as preliminary results, since there is no data to validate the model at the time of the GLO survey, and since it is the first time that Cuencas is used to model the effects of land cover in Iowa's hydrology. However, the potential large reduction on discharge of the pre-settlement land cover is an incentive to investigate this issue further and continue developing Cuencas to capture the effects of less drastic land cover changes.

TABLE OF CONTENTS

LIST OF TABLES

LIST OF FIGURES

INTRODUCTION

The large flooding experienced in Iowa in June of 2008 made the state realize that there was a need to have a fast and reliable tool to predict flooding, even in the absence of functioning stream gauges. To respond to this need, the Iowa Flood Center of the University of Iowa, is developing Cuencas, a hydrological model that in a short time can predict the water discharge at different locations in a watershed, even in ungauged streams. Cuencas started to be developed several years ago, but it is being adapted to fit Iowa's watersheds and to predict accurately and in real time the discharge in small and large (state level) watersheds. This study had as an objective to use Cuencas to model the discharges of June 2008 in the Turkey River Watershed at Eldorado and Elkader, which encompasses 900 mi^2. The results from this study were used to test the performance of Cuencas modeling this event at this scale, contributing to the overall development of this tool.

Another objective of this study was to give some light into the role that the drastic land cover change of Iowa's watersheds had in the 2008 flooding. This study used a version of Cuencas modified by Luciana Cunha (Cunha's Model) that includes the effects of land cover in stream discharge to explore the possible role that the land cover conversion had in the floods of 2008 at Elkader, Iowa. The model was run using the 2008 rain event and the land cover of the Turkey River watershed present before European settlement (1832-1859) and the 2001 land cover. The predicted discharge under both land covers was compared as an indication of the effects of land cover in the floods experienced. Since a flood event is the result of many factors that vary in space and time, the results of this study only apply to Elkader and Eldorado, Iowa, and to the rainfall conditions present in June 2008. However, this study can be used as a framework to investigate other rainfalls and other land covers and can give some insight into the effects of land cover conversion on flooding.

CHAPTER I: LITERATURE REVIEW

1.1 Land use land cover change in Iowa

Iowa's ecosystems have been drastically modified. Among the 50 states of the United States, Iowa has lost the highest percentage of its native vegetation due to agriculture. Since the European settlement in the 1830's, vast prairies and woodlands have been replaced mainly by corn and soybeans, and wetlands have been drained. Iowa's land use and land cover (LULC) has changed from a mixed landscape that included prairies, woodlands and wetlands to a predominantly agricultural landscape with corn and soybeans covering more than 70% of the state (U.S. Census Bureau 2009). It is estimated that 89% of wetlands have been drained in the state (Mitsch & Gosselink 2007), the second highest rate of wetland loss after California (91% loss). Even though the total land cultivated with corn has not increased significantly in the last 50 years, there has been significant conversion of pastures to soybean production, which has resulted in increased of total area dedicated to row crops (Jackson & Keeney 2010).

1.2 Effects of Iowa's land use land cover change on hydrology

LULC changes affect the partitioning of rainfall into the different components of the hydrological cycle (e.g., evapotranspiration, infiltration, and runoff), altering flood generation processes. LULC changes are frequently the result of agriculture intensification, urban development and/or deforestation.

In Iowa, the intensification of agriculture has caused most of the LULC changes. To obtain the current agricultural landscape it was necessary to construct artificial drainage systems (subsurface tiles and surface ditches), drain wetlands, modify stream courses, fill floodplains and of course, change the vegetation.

The change of vegetation alone has many implications in the hydrology of the land. The pre-agricultural heterogeneous vegetation structure of native prairies and woodlands intercepted water and slowed down overland flow. In the contrary, the current homogenous vegetation of row crops routes precipitation rapidly to artificial drainage networks and streams as runoff. Bharati et al. (2002) found that the cumulative infiltration for multi species buffers that replicate the pre-agricultural landscape were five times larger than the infiltration for crops and pastures. Also, Prairies may intercept 10 times more precipitation than row crops (Brye et al. 2000), and therefore prairies have a lower runoff potential than crop fields. In addition, the water demands of young corn/soybean plants and pasture are lower than the water demands of mature prairie plants or trees. Most important, the lack of vegetation from the late fall until the spring (approximately half of the year) in the agricultural landscape makes it easy for water to reach drainage ditches and streams rapidly during the spring snow melt and rainfalls, via direct runoff or via tile drains (Bharati et al. 2002). All the factors described above result in higher rates of rainfall-runoff transformation (or tile flow in tiled watersheds) and in shorter times of concentration in agricultural/pastoral systems than in prairies and woodlands.

Another impact that the change of vegetation can have in the hydrology of an area is the reduction of the water retention capacity of the soil and the reduction on the evapotranspiration potential of the plants. The maximum rooting depth of temperature deciduous trees is larger than the depth of temperate grasslands (including prairies and pastures) and that the depth of croplands (Canadell et al. 1996). In addition, tallgrasses of the native Iowa prairies have a higher density of fine roots than corn and soybeans (Tufekcioglu et al. 1998; Craine et al. 2003). Since rooting depth and fine root density are directly correlated with increased water retention capacity and increased rates of evapotranspiration (Zhang et al. 2001; Asbjornsen et al. 2007) it is clear that with the vegetation change (from trees to pastures and from tallgrass prairie to corn and soybeans), the evapotranspiration and water retention capacity of the soil in the agricultural Iowan landscape have been largely reduced.

In summary, the transformation of native landscape to agriculture, which includes replacing perennial vegetation (prairies and woodlands) for annual crops and pastures, creation of artificial drainage networks, wetland draining and modifications to floodplains and stream channels, has decreased the water retention capacity of the soil and the evapotranspiration potential and water interception of the vegetation, resulting in higher runoff and tile flow, and in lower times of concentration. Tiling has modified the hydrology significantly in Iowa, and in some cases the tile flow component of the baseflow (as opposed to ground water) has been measured to exceed 70% (Schilling & Helmers 2008).

During the second half of the twentieth century, annual streamflow, annual baseflow, and annual minimum flow have increased in several watersheds in Iowa and in the Mississippi river basin, which may be attributed to the conversion of perennial vegetation to row crops (reducing evapotranspiration and leaving more available water for runoff or infiltration) and the installation of artificial drainage on crop lands (transporting surface water and tile water fast to streams) (Schilling & Libra 2003; Schilling 2005; Zhang & Schilling 2006).

The effects of the land cover change in flooding are also relevant. For instance, the increase of runoff and tile drain in Iowa has increased the number of streams and the stream flow, and therefore, it has increased the stream erosion capacity (Burkart 2010). As result, more sediment is deposited in flood control features and streams, reducing their water storage and conveyance capacity, and increasing flood risks. The time of concentration has decreased as a consequence of the land surface becoming smoother, and the creation of aboveground and underground water paths (artificial drainage systems) that offer a reduction of the resistance to the flow. This also has resulted in higher peak flows and therefore in higher flood risks (Andersen et al. 1996; Burkart 2010).

To determine the effects of one of these landscape modifications in a basin hydrology is complex, since many of the factors are interconnected. For instance, in most cases it is not possible to determine if hydrologic, water quality and ecologic impacts observed are due to tiling (subsurface drainage) or to other changes associated with agriculture (Skaggs et al. 1994; Blann et al. 2009).

The quantification of the hydrological effects of converting prairie to crops is difficult. There are several papers describing and quantifying some of the effects of this land cover change (Bharati et al. 2002, Brye et al. 2000, Burkart 2010), but besides the Curve Number tables of the Natural Resources Conservation Service (Mishra & Singh 2003) there is no published data quantifying the rainfall/runoff transformation expected from a prairie field versus a field planted with corn.

It is especially difficult to quantify the effects of the LCLU change at large scales, which generates controversy on the effects that the land cover transformation has had on flooding probabilities in Iowa. To help clarify these effects the use of hydrologic models is necessary.

1.3 Basin scale hydrologic models

There are many types of basin scale hydrological models, including statistical models and physically-based models.

Statistically based models attempt to fit statistical distributions to historical data. For instance, in the case of ungauged basins or when data for the study basin is not available, regression equations are used to estimate the basin's hydrologic responses, including the peak flow, as a function of the basin's physical attributes. These models are based on correlations, and not on cause and effect (like the physically based models), which makes them not appropriate to describe non random variables like streamflow.

Physically-based models are not based on correlations, but on causes and effects. They use equations that are developed based on the physics of the processes that they describe. These models link inputs (e.g., hydro meteorological data) with the response of the stream network and other components (like sub surface water) to these inputs. These models often require large computational resources to find numerical solutions to their equations. Several of these models can link hydrology with sediment and pollutant transport in the watershed.

The majority of the current physically-based models are complex. They try to capture many of the processes that the modeler considers determine the hydrology outputs at the different scales. This approach requires large amount of data, high demand in computational resources and complex statistical and mathematical analysis (Sivakumar 2008). Many of the physically-based models available divide the watershed in smaller user defined units that may not correspond to the scales for which physical equations were developed. Also, since these models are often developed to fit specific situations, and since the data required to feed the models is not always available, calibration of model parameters is required to obtain results (Cunha et al. 2011).

A different approach to hydrologic modeling is the Data Based Mechanistic (DBM) modeling method (Young 2002). This approach performs a statistics analysis to define the parameters in which a physically-based model should be developed, as opposed to use all the parameters that the modeler considers relevant. By using this approach the number of parameters used in the model can be significantly reduced, possibly eliminating interactions between parameters that can produce erroneous results (Jackson et al. 2008; McIntyre & Marshall 2010).

Another alternative to complex modeling approaches, are parsimonious models that instead of attempting to capture everything in the watershed, capture the essential features in the watershed (e.g., the model uses as few parameters as possible to obtain acceptable results) (Sivakumar 2008). As opposed to DBM that start with many parameters and discard parameters that are not relevant, parsimonious models start with the least amount of parameters and include more parameters if necessary. One example of these parsimonious models is Cuencas (which means Basin in Spanish) (Mantilla & Gupta 2005). Cuencas is being developed at the University of Iowa's IIHR-Hydroscience and Engineering and is being used to simulate the hydrology of different watersheds. Cuencas will be described in more detail in section 3.2.

There are many hydrological models that can be applied at the watershed scale, but unfortunately their applicability and limitations are not always clear, making it difficult to choose the best model to use for a specific study. To help in the selection of models, several authors have made comparisons between several models (Kokkonen 2003; Borah & Bera 2004; Singh & Frevert 2006). Four of the most widely used physically-based hydrological models for large-scale watershed modeling are described below.

HEC-HMS, is the Hydrologic Modeling System developed by the US Army Core of Engineers (Feldman 2000). HEC- HMS is a lumped hydrological model designed to simulate rainfall-runoff transformation process of dendritic watersheds. HEC-HMS can be used in small urban watersheds or in large basins. It divides the hydrological cycle in different processes and uses mathematical models to represent the fluxes of mass and energy in the watershed.

GSSHA, the Gridded Surface Subsurface Hydrologic Analysis (Downer et al. 2006), was also developed by the US Army Core of Engineers. As opposed to HEC-HMS, GSSHA is a distributed hydrological model, allowing the user to enter different parameters at the grid scale. GSHHA has a coupled groundwater and surface water component. GSSHA can model the transport of chemicals and sediment, besides the transport of water. GSSHA can be used to simulate single events or long term hydrological processes.

SWAT, the Soil and Water Assessment Tool (Arnold et al. 1998) was developed by the US Department of Agriculture (USDA). SWAT is a continuous simulation model that was developed to simulate the impact of different management practices on water, sediment and chemicals in agriculture dominated watersheds. The hydrological model component uses the Soil and Conservation Service Curve Number (SCS-CN) to link runoff processes and land use. SWAT is a lumped model and divides the watershed in user-defined Hydrologic Response Units (HRUs). SWAT was developed for long-term predictions of flows and most of its applications have a daily time step, therefore this model is not appropriate for detailed simulations of single events. For instance, Reungsang et al (2005), found that SWAT was not able to accurately predict daily peak flows, however it accurately predicted monthly flows at the Upper Maquoketa River watershed.

MIKE-SHE (Graham & Butts 2006), a modification of the European Hydrological System Model, is another commonly used distributed physically-based model to simulate hydrology at a watershed scale. MIKE-SHE can simulate the transport of water, sediment and chemicals, between the surface, soil and groundwater. MIKE-SHE can be used for single events or for long-term simulations of hydrological processes.

One of the main challenges when using the models described above is that all of them require the input of extensive data (to define numerous parameters), which may be not available, and therefore calibration is required. Also, the lumped models described (SWAT and HEC-HMS) do not recognize the spatial variability of some processes, and the distributed models (MIKE-SHE and GSSHA) use the grid as their unit, which does not necessarily correspond to the scale at which the physical equations were defined.

Therefore a model with the least number of parameters required to produce adequate results (i.e., a parsimonious model), and that applies physical equations to the scales for which these equations were formulated, might offer the best option when analyzing the effects of different management strategies, or climate change scenarios in watershed modeling. Having less parameters and data entry also should reduce the computational resources needed, which is necessary when fast and reliable simulations need to be run at large watersheds (like state-wide). Cuencas has this characteristics and it will be described in Section 3.2.

CHAPTER II: STUDY AREA

2.1 Basin description

The study area corresponds to the Turkey River Watershed (basin) at Elkader, Iowa. The basin lies in northeast Iowa in the counties of Howard, Chickasaw, Winneshiek, Allamakee, Fayette and Clayton. The basin is approximately 2,300 km^2 (900 mi^2). The main river tributary to this basin is the Little Turkey River, which joins the Turkey River north from Eldorado, Iowa (Figure 1).

There are two landforms that define the geomorphology of the watershed. The northwest part of the watershed lies within the Iowan Surface and the southeast part of the watershed lies within the Paleozoic Plateau. The Iowan Surface is characterized by long slopes and low relief with subtle stepped levels that mark watershed divides (Prior 1991). Drainage networks are well established, with low stream gradients, and it has some poorly drained areas where wetlands exist. There are large fieldstones known as glacial erratics, sinkholes, and deposits of limestone and dolomite. Due to the carbonate rocks, there are rock aquifers that sustain rivers in dry conditions. This zone of the watershed is mostly cultivated. The Paleozoic Plateau is characterized by the steepest landscape in Iowa. The topography of this zone is controlled by the bedrock, and therefore it is deeply carved with a high relief. It has deep, narrow and steep river valleys with meander patterns and fast flowing streams. This region is also characterized by kharst topography, containing many sinkholes, caves and springs underlined by dolomite and limestone. This zone contains a high percentage of the native woodlands of the state, since there are steep areas unsuitable for cultivation (Prior 1991).

The Government Land Office (GLO) did a vegetation survey of the area between 1832 and 1859. According to these records 58% of the basin was covered by prairies and 42% of the basin was covered by woods before European settlement (Figure 2). The present land cover consists of row crops in almost 63% of the basin, followed by pastures

(13%), woods and grasslands (including prairie remnants') (8%), developed areas (6%) and water (streams and wetlands) (1%) (Figures 3 and 4).

Even though the main land cover conversion in the Turkey River Watershed occurred before 1875 (Wehmeyer et al. 2011), the total land area dedicated to row crops in Northeast Iowa increased during the 20th century, especially with the introduction of soybeans in the seventies, and it seems to have reached an almost stable level in the last decade (USDA 2011) (Figure 5).

2.2 Flooding history

Currently, there are two United States Geological Services (USGS) gauges that keep 15-min stage and discharge measures in the basin, located at Eldorado and at Elkader (Figure 1). A third station located at Spillville keeps daily stage measurements. The location of the USGS gauging station at Elkader slightly changed. The USGS station 05412000 (drainage area of 891 square miles) has streamflow records from 1916 to 1942. The new station (05412020) is located above French Hollow Creek has a drainage area of 903 square miles and has records for 1991, and from 2002 until present. The USGS Station at Eldorado (05411850) has a drainage area of 641 square miles, and has streamflow data since September of 2000.

The largest flood recorded in Elkader was in June, 2008, with a stage of 27.77' and a discharge over 40,500 cfs. This 2008 flooding event is followed in magnitude by an event on June 1991, which had a stage of 27.32' and a discharge over 38,000 cfs. A third significant event occurred in May 2004, when the peak flow was 25.57' and the discharge over 33,000 cfs. The largest discharge recorded for Eldorado was 50,100 cfs in 2008, followed by 2004 (19,700 cfs) and 1991 (16,700 cfs) (Figure 6). Flood hydrographs for the 2004 (Figure 7) and 2008 (Figure 8) events were created using the continuos data available at the Instantaneous Data Archive of the USGS (USGS 2011a).

Since the USGS stations of Eldorado and Elkader do not have long and continuos records, data from the USGS station at Garber (05412500) (drainage area of 1545 square miles) downstream of Elkader in the Turkey River Watershed (but outside of this study basin) and from the USGS station at Maquoketa (05418500) in Maquoketa River Watershed (drainage area of 1553 square miles) were analyzed, given that these watersheds are nearby and have comparable size (Figure 9). It appears that the largest peaks observed in the Turkey River Watershed have occured in the last two decades (Figure 10). The Maquoketa station has records of significant flooding events since the 1900, but the more severe events have occured in the last 50 years (Figure 11).

Figure 12 contains the Flood Insurance Rate Map for Elkader created by the Federal Emergency Management Agency (FEMA) and last updated in 1996 (Federal Emergency Management Agency (FEMA) 2011). The grey area corresponds to the 100-year floodplain and the dashed area corresponds to the floodway, which includes the channel and the zone that conveys flood waters with higher speeds. This map shows the areas that are more vulnerable to flooding in the city, but does not imply that the areas that are not shaded are not at risk for flooding. The Iowa Flood Center is working on updating this flood map using the information generated after the floods of 2004 and 2008.

Figure 1. Turkey River watershed at Elkader, Iowa (study basin)

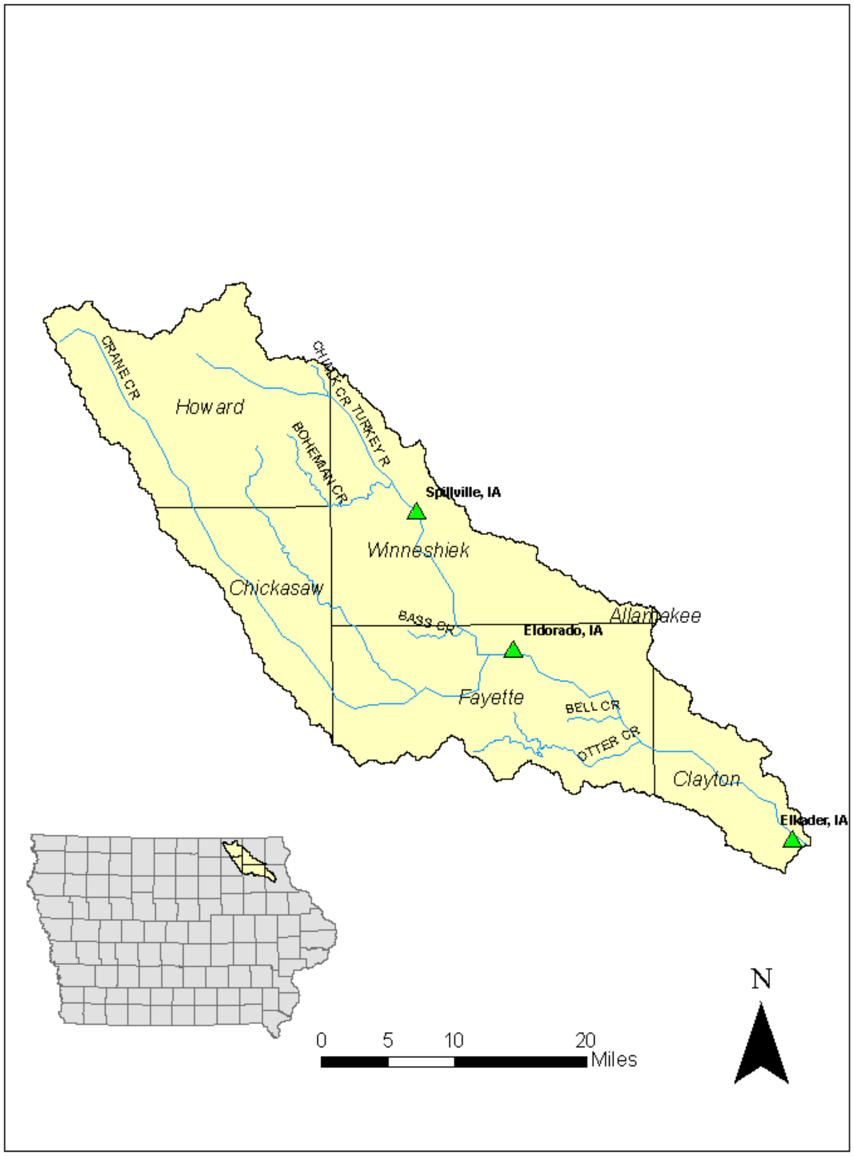

Figure 2. Basin land cover during the Government Land Office Survey

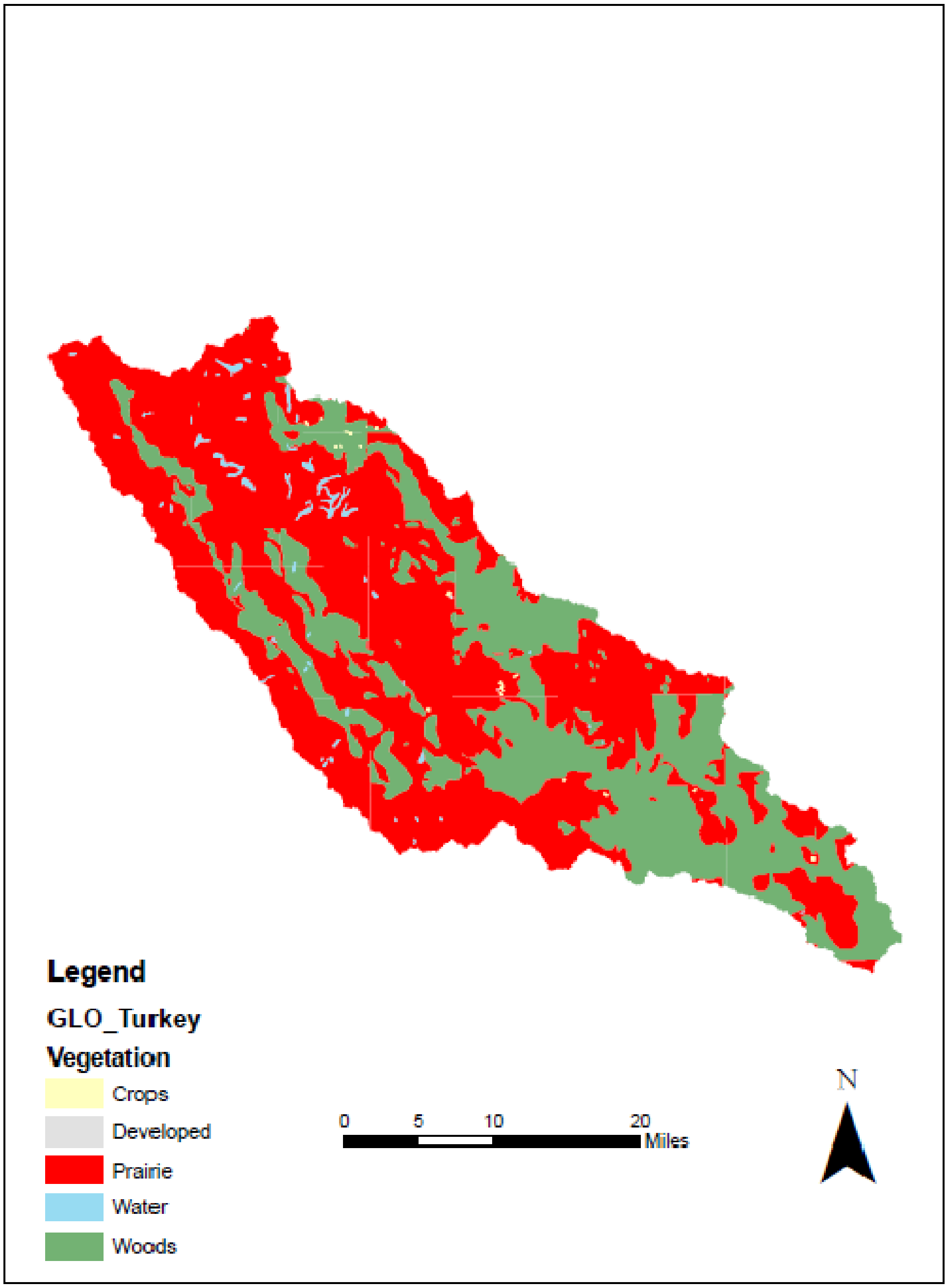

Figure 3. Current (2001) land cover in the basin

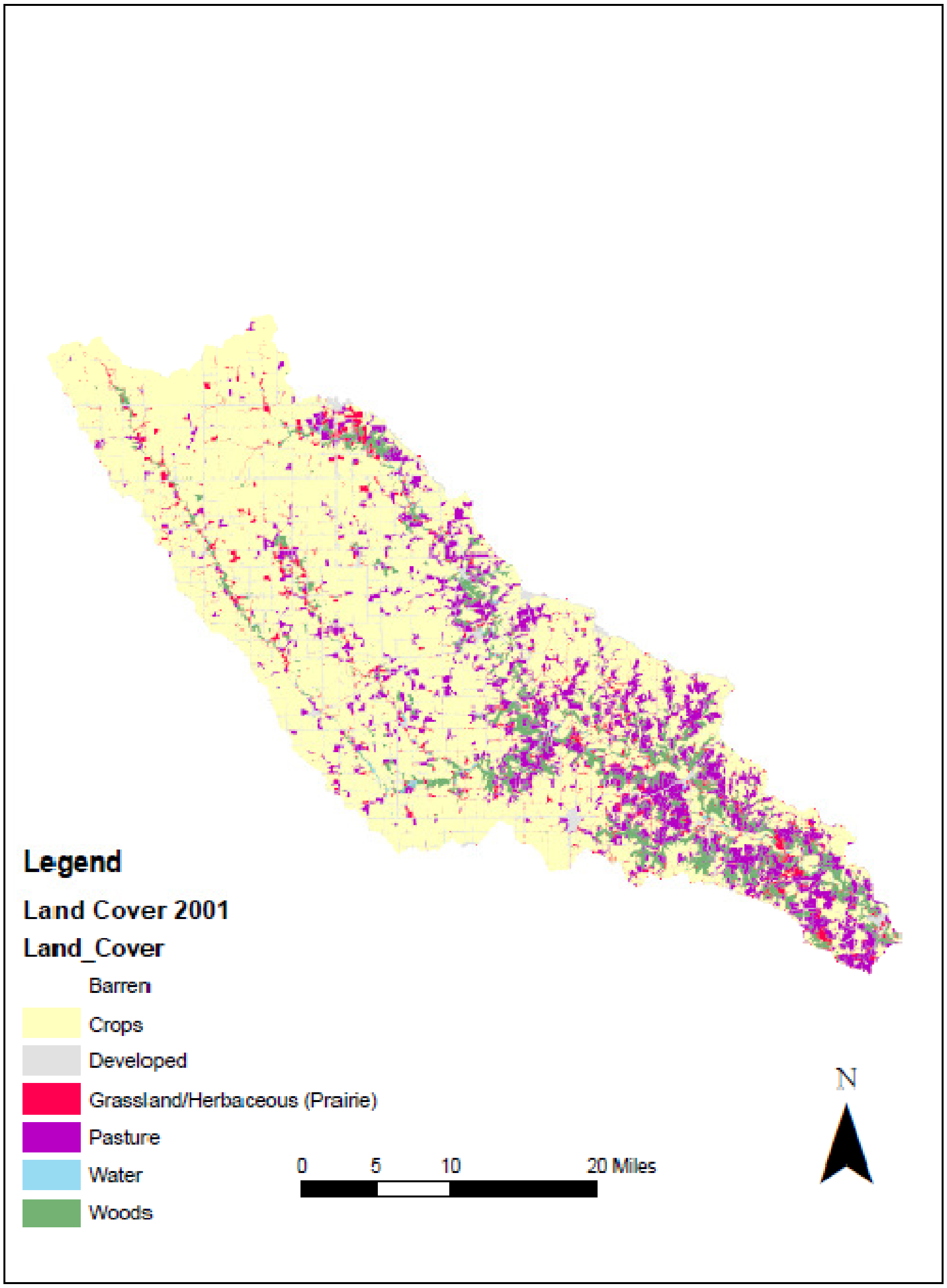

Figure 4. Land cover comparison between 1832-1859 and 2001

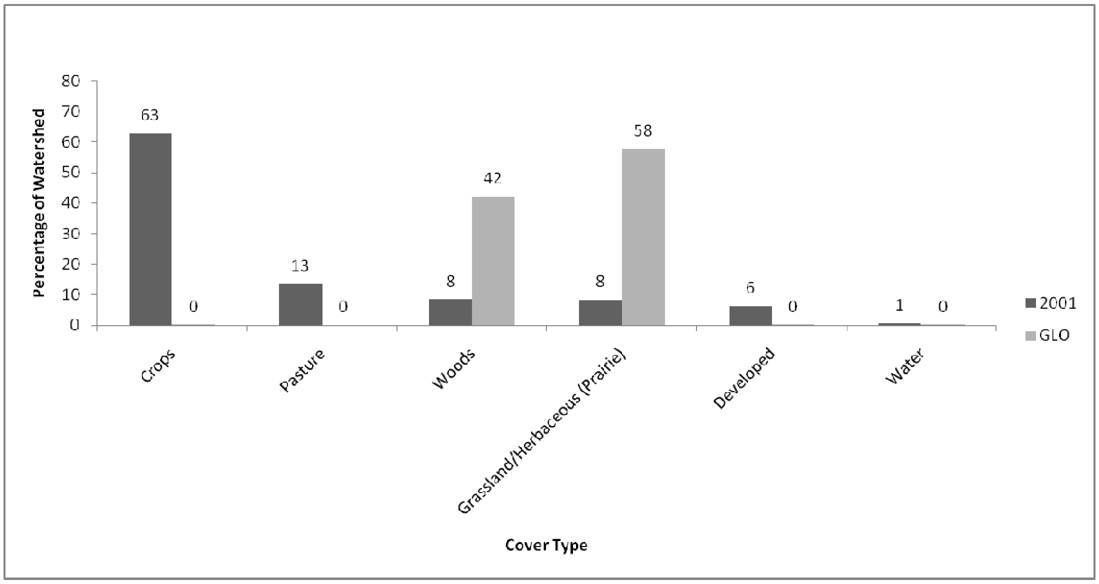

Figure 5. Area cultivated in corn and soybeans in northeast Iowa

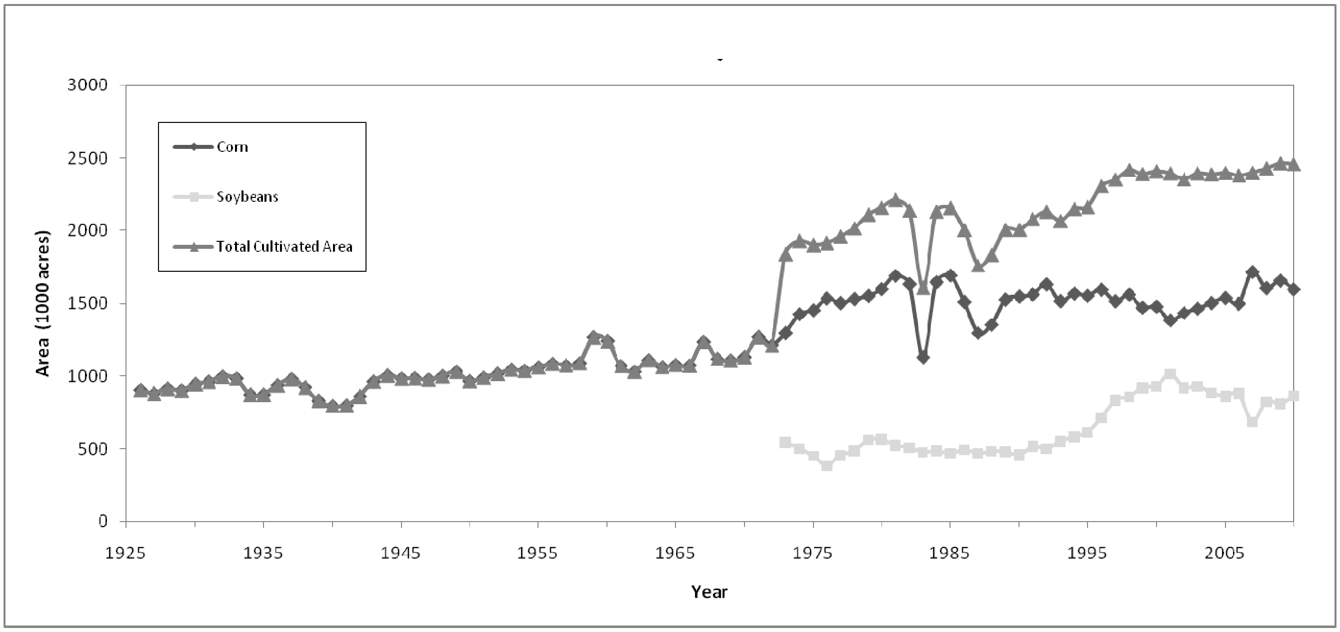

Figure 6. Peak flow records recorded at Eldorado and Elkader

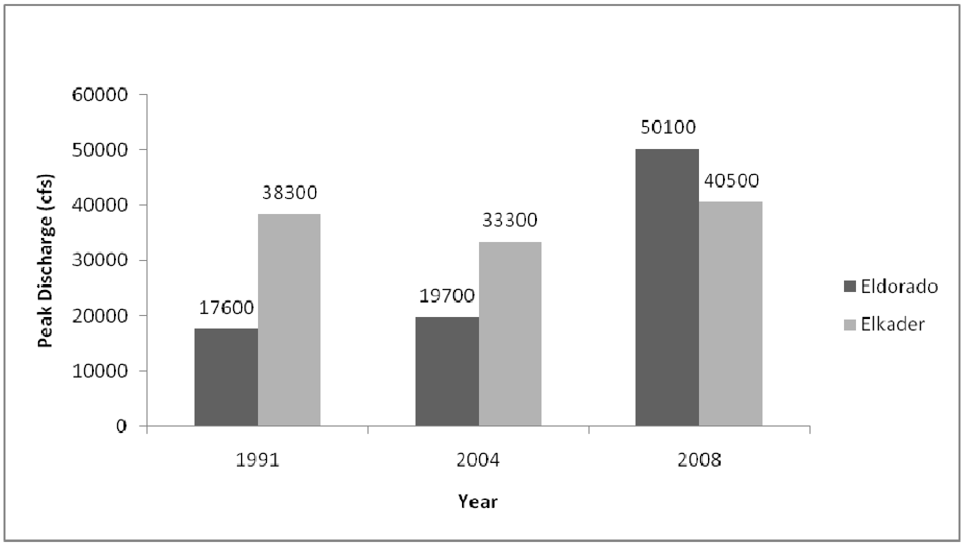

Figure 7. Hydrographs of the flood of 2004 at Eldorado and Elkader

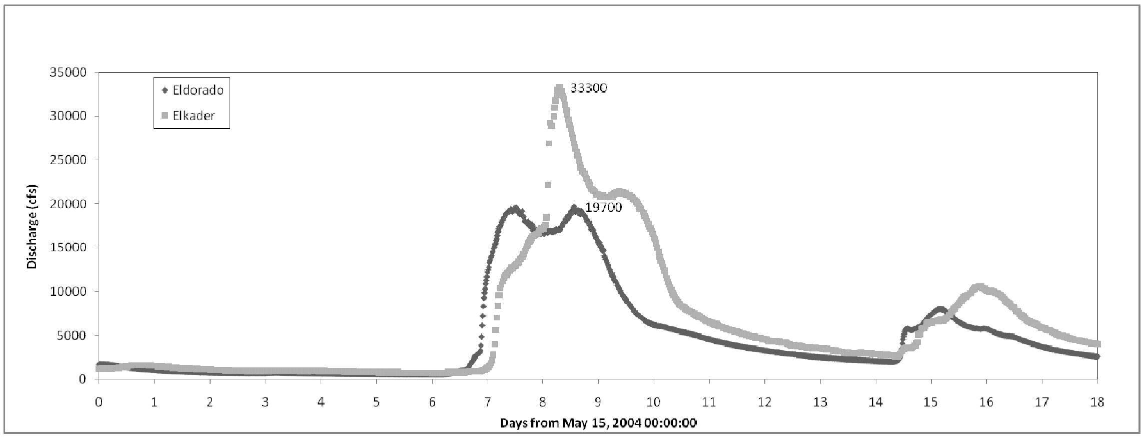

Figure 8. Hydrographs of the flood of 2008 at Eldorado and Elkader

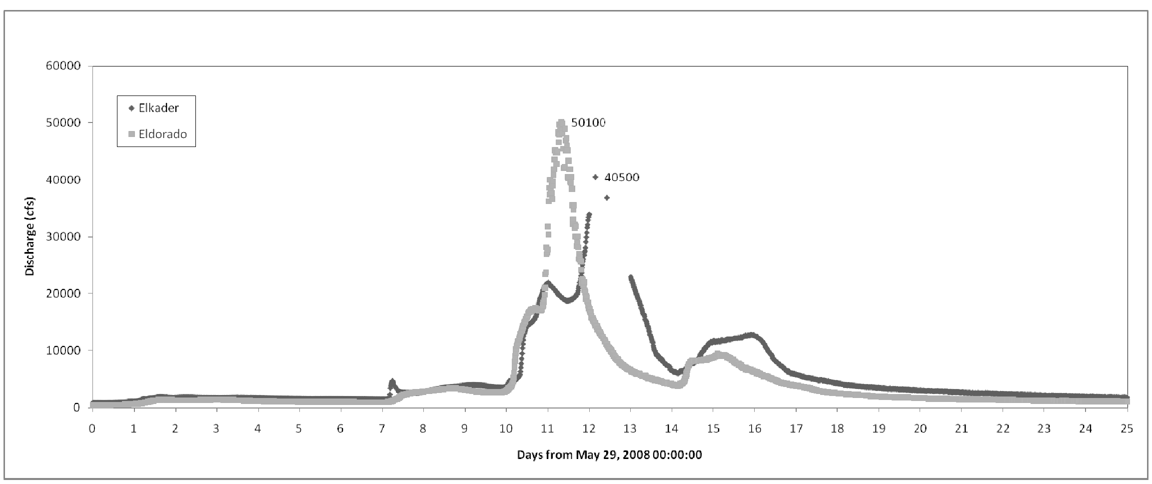

Figure 9. Watersheds and USGS stations located in or nearby the study basin

Figure 10. Historical peak flood discharges at the Turkey River Watershed

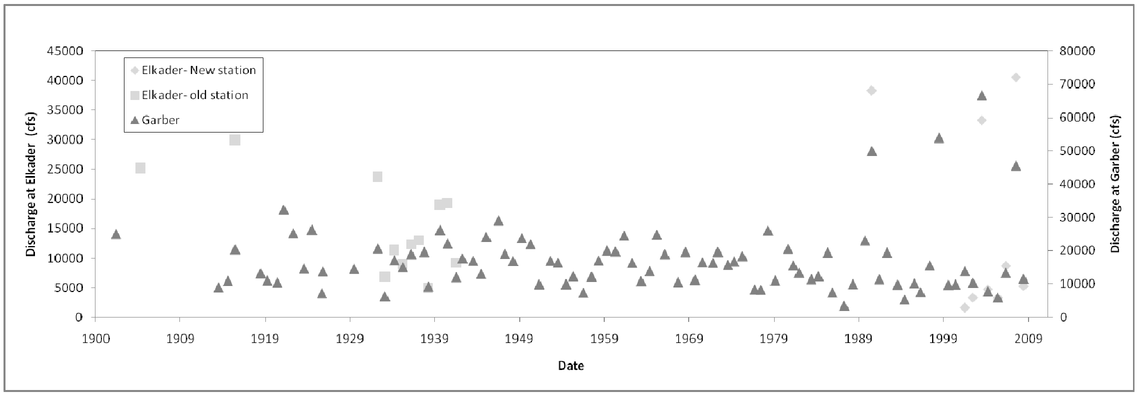

Figure 11. Historical peak flood discharge and stage at the Turkey River (at Garber) and Maquoketa River (at Maquoketa) watersheds

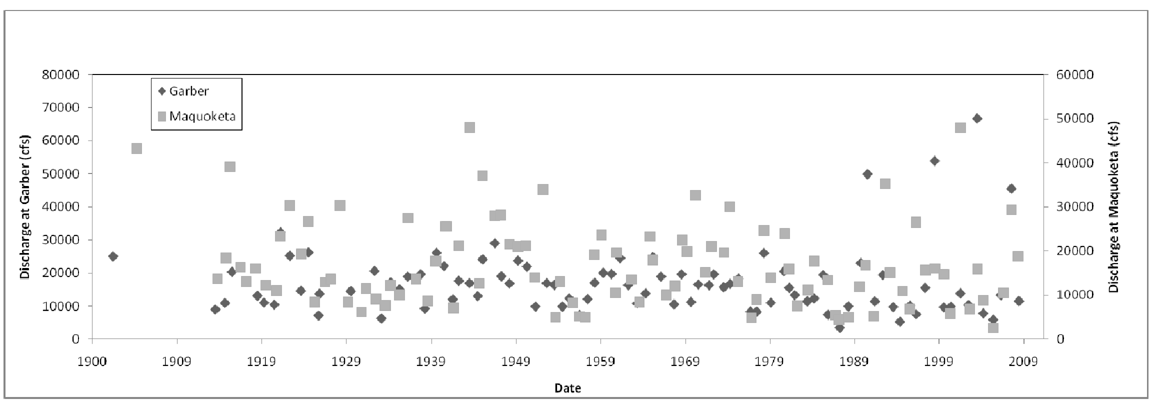

Figure 12. Flood Insurance Rate Map for Elkader, Iowa

CHAPTER III: STUDY DESCRIPTION

3.1 Justification and objectives

The main cause of recent large flood events in Iowa is a reason of considerable debate. One argument is that the main cause of the extreme flooding events are the modifications to the landscape, including wetland drainage, floodplain filling, agricultural tiling and change of vegetation.

Another argument is that the floods are the result of extreme rainfall events, and that tiling might help avoid large flooding. This is justified by arguing that a tiled field reduces overland runoff (reducing the sediment load of runoff and therefore the sedimentation of stream channels and flood control features), and increases the infiltration capacity of the soils. It is also argued that a tiled field keeps a field from freezing when it is moist, and therefore the field has more absorbing capacity when the spring melt occurs (Love 2010; Zingula 2010). Even though these arguments may be valid at the field scale under certain soil, rainfall, topography and drainage conditions, they cannot be translated to the watershed scale (Smedema et al. 2004; Blann et al. 2009). It is true that the overland runoff can be reduced when subsurface drainage is present (as compared to overland runoff of a surface drained field), but the tile flow increases and it reaches the streams faster than groundwater flow, which also contributes to peak flows.

The effect of the rainfall on the floods of 2008 was explored by Krajewski and Mantilla (Krajewski & Mantilla 2010). They concluded that the individual events were not so extreme, but the combination of events during the one to three week time span proceeding the crest significantly surpassed the mean annual maximum precipitation across the state. They also attributed large flooding in the Cedar and Iowa River basins to the spatial and temporal distribution of the rainfall.

Reports from the National Oceanic and Atmospheric Administration (NOAA) agree that the total observed rainfall in the spring and early summer of 2008 was extreme.

June of 2008 has been the second wettest June in record in Iowa, and the period from April to June was the wettest recorded (NOAA Satellite and Information Center 2008). The monthly precipitation records for 1993 were also considered extreme and this accumulated precipitation (not a single event) was deemed as the main cause of large flooding in the Midwest of the United States (Guttman et al. 1994).

On the other hand, the effect of LULC change on these large flood events has not been studied. Several studies in other watersheds and flooding events suggest that LULC does have an effect on stream peak flows, which are responsible for flooding (Fitzpatrick et al. 1999; Hejazi & Markus 2009). For instance, a study comparing the effects of increasing precipitation and LULC change in increasing flooding in four watersheds in Illinois, attributed most of the variability of the increase in peak flows to the LULC (and drainage) change and not to the increase in precipitation (Changnon & Demissie 1996).

The objectives of this study are to evaluate the suitability of Cuencas as a tool to model the 2008 flood event in the Turkey River Watershed at Elkader and Eldorado, and to explore the role that LULC change had on the 2008 floods in this basin.

The driving hypothesis of this work is that even though the extreme precipitation from April to June of 2008 would have caused large flooding under any land cover, the extent of the flooding would have been lower under a pre-settlement land cover, and that this would be more dramatic at the beginning of the event, before the soils were saturated.

3.2 Model description

Cuencas is described as a calibration-free, parsimonious hydrological model, and it has been used to model from single hillslopes to large (of the order of thousands of kilometers squared) watersheds. Cuencas is a river network simulation environment initially developed by Mantilla and Gupta (2005). Cuencas includes GIS based tools that use high resolution Digitally Elevation Models (DEMs) to extract the river network and decompose the landscape into links and hillslopes. A link is defined as a section of a channel between junctions, between a source and a junction or between a junction and an outlet. Links are usually from 200 to 500 meters long. A hillslope is the area of the terrain that drains directly into the link, and vary from 0.01 to 0.1 km^2. Cuencas uses the D8 algorithm (maximum gradient method) to obtain a drainage direction matrix, and prune algorithms to obtain the location of the river network (O'Callaghan & Mark 1984).

A characteristic that differentiates Cuencas form other GIS based hydrological models, is that it uses the hillslope as the basin partitioning unit, and not arbitrary subwatersheds, grids or pixels. This is important since it is at the hillslope scale where rainfall-runoff partitioning occurs, and therefore Cuencas is able to apply physically-based equations of rainfall-runoff partitioning at the scale at which they occur.

Cuencas models the two main processes affecting the response of a watershed to rainfall: the partitioning of rainfall into runoff at the hillslope scale and the transport of flow downstream in the network. Cuencas is a modeling framework that allows the modification of the equations that it uses. For instance, as a first order approximation Cuencas assumes a constant runoff coefficient and stream velocity in space and time. However, since this is not appropriate to analyze the effect of land cover on flooding, the model was modified by Luciana Cunha (Cunha's Model) to include a land cover component (Cunha et al. 2011).

Cunha's Model uses the same equations from the first order approximation for the transport of water, but it uses the SCS-CN method to determine the rainfall/runoff transformation (instead of using a constant runoff coefficient), and adds components to model the transport of the infiltrated water in the subsurface, through the vadose (unsaturated) zone and saturated zone to the channel.

3.2.1 Transport of flow

The transport of water in the stream network is the governing factor on the response of a watershed to rainfall at a large spatial scale, and it is determined by the mass conservation equation of flow developed by Gupta & Waymire (1998):

$$\frac{dS(t)}{dt} = aR(t) + q_1(t) + q_2(t) - q(t)$$

Where *S(t)* is the storage in the link at time *t*, *a* is the area of the hillslopes draining to the link, *R(t)* is the runoff intensity per unit area produced by the hillslopes draining to the link, $q_1(t)$ and $q_2(t)$ are the incoming flows of the two upstream tributaries, and *q(t)* is the flow rate at the outlet of the link.

Flow discharge (*q*) and channel storage (*S*) can be written as:

$$q = v \times C_A$$

$$S = l \times C_A$$

$$S = \frac{l}{v} \times q$$

It is assumed that the depth of the link does not change across the link during time *t*. C_A is the link average cross section (assumed to be rectangular, equal to width times depth), l is the link length and v is the link velocity.

The velocity in the link and is defined as (Mantilla 2007):

$$v(q) = v_0 \times q^{\lambda_1} \times A^{\lambda_2}$$

Where v_0 is the initial velocity, *q* is the channel discharge, *A* is the drainage area, and λ_1 and λ_2 are scaling exponents.

These scaling exponents λ_1 and λ_2 can be estimated if the velocity, discharge and area are known and the variables of the previous equation are log transformed:

$$\log (v) = \log(v_0 \times q^{\lambda_1} \times A^{\lambda_2})$$

$$\log (v) = \log(v_0) + \log\left(q^{\lambda_1}\right) + \log(A^{\lambda_2})$$

$$\log (v) = \log(v_0) + \lambda_1 \log(q) + \lambda_2 \log (A)$$

To find v_0, λ_1 and λ_2 a multivariable linear regression using regional data can be done applying the last equation.

The discharge of each link in the river network is obtained with the following nonlinear differential equation proposed by Mantilla et al. (2006):

$$\frac{dq}{dt} = K(q) \times [aR(t) + q_1(t) + q_2 (t) - q(t)]$$

Where K is defined by the solution to the momentum equation:

$$K(q) = \frac{v(q)}{l\,(1 - \lambda_1)}$$

3.2.2 Partition of rainfall into runoff

The first order approximation uses a constant runoff coefficient to model the rainfall transformation into runoff.

$$R(t) = RC \times P(t)$$

Where $R(t)$ is the runoff at time t, RC is the runoff coefficient, and $P(t)$ is the precipitation at time t.

This assumes that the percentage of the rainfall that will become runoff does not change in space and time. In a large watershed scale, the runoff coefficient does vary in space and time, however the main process affecting the response of the watershed to rainfall at a large scale is the transport of water in the river network, and not the rainfall-runoff transformation (Cunha et al. 2011), and therefore the results might not change much when adding a complex runoff-rainfall transformation process to the model.

However, in cases where the partition of rainfall on runoff wants to be studied, such as when the role of land cover in flooding is to be explored, it is necessary to use a different method to model the runoff generating process. The objective of Cunha's Model is to account for the variation of the rainfall/runoff process in the model results.

The temporal and spatial variability of runoff coefficients is caused by the spatial and temporal variability of physical characteristics (land cover, soil type, land management, etc) and by the temporal variability of different factors, including soil moisture conditions (affecting the ability of soils to infiltrate and retain water) and the ability of plants to transpire water.

The Curve Number methodology was developed by the Soil Conservation Service (currently the Natural Resources Conservation Service) as a simple way to model the rainfall/runoff transformation. The Curve Number (CN) represents the capability of soils to produce runoff, and its value depends on land cover, land use management, soil type and antecedent soil moisture condition (AMC). The CN method assumes proportionality between runoff and retention: Actual Runoff (Q) is to Potential Runoff (P, equal to Precipitation) as Actual Soil Moisture Retention (F, equal to P-Q) is to Potential Soil Moisture Retention (S) (Ponce & Hawkins 1996):

$$\frac{Q}{P} = \frac{F}{S}$$

The runoff equation of the CN is:

$$Q = \frac{(P - Ia)^2}{P - Ia + S}$$

Where Q is runoff, P is rainfall, S is the potential maximum soil moisture retention after runoff begins, and Ia is the initial abstraction, or losses before runoff begins (including water intercepted by vegetation, water stored in surface depressions, evaporation, infiltration).

CN and the potential retention (*S*) are related by the following equation:

$$S = \frac{1000}{CN} - 10$$

The CN for average runoff conditions and for an Initial abstraction equal to 20% of the potential soil retention (average for agricultural watersheds) can be obtained by looking at the Runoff CN for hydrologic cover complexes tables developed by the Soil Conservation Service (Mishra & Singh 2003). Typical values of CN vary from 30 to 100. A low CN indicates low runoff potential while a large CN indicates a large runoff potential.

Since the capacity of the soil to retain water changes with time, decreasing as the soil gets saturated and increasing as the soil dries, the CN method takes into account the Antecedent Soil Moisture Condition (AMC) to determine the CN. There are three classes of AMCs. AMC I correspond to dry soils, AMC II to average runoff conditions, and AMC III to saturated soils. The rainfall of the previous five days determines which AMC should be used (Table 1).

Cunha's Model uses four differential equations to model the overland runoff (*dq/dt*), the subsurface water (*dS/dt*), the movement of infiltrated water in the vadose zone (*dθ/dt*), and the water movement in the saturated zone (*dλ/dt*). This model assumes that the shape of the underground water storage layer mirrors the shape of the hillslope, and models the vadose and saturated zone as linear reservoirs using Darcy's equation.

There is a variable contributing hillslope area of runoff to the channel, which is composed of a permeable area and an impermeable area. The permeable area is the surface area that is over the vadose zone and the impermeable area is the surface area that is over the saturated zone (Figure 13). The effective precipitation (precipitation minus losses due to transpiration, or to overland storage) can either be transformed in runoff or be infiltrated. The water that is infiltrated can either travel underground to the saturated zone or be go to the bedrock, and the water that is in the saturated zone can recharge the channel or go to the bedrock as well (see arrows in Figure 13). The equations used in this model will be published in Cunha's Ph-D dissertation.

3.3 Model inputs

3.3.1 Topographic information

A 1-arc second (approximate 30 meters) DEM was obtained online from the USGS (USGS 2010b). To decrease modeling time, this DEM was transformed using Arc-GIS to a 3-arc second DEM (approximate 90 meters). Cuencas was used to extract the river network and decompose the terrain into links and hillslopes using this DEM. The extracted river network by Cuencas can be found in Figure 14.

3.3.2 Land cover information

To make the comparison between different land covers, the existent land cover from 2001 and from the time of the General Land Office Survey (GLO) (1832-1859) were used. The 2001 National Land Cover Data was obtained from the USGS Seamless data warehouse. The GLO vegetation information was obtained online from the Iowa DNR (IA DNR 2011). Since the 2001 and GLO land covers had different classifications, the GLO information was transformed to the codes used in 2001 (Table 2).

3.3.3 Soil type

The hydrologic soil type was obtained online from the SSURGO Database (Natural Resources Conservation Service (NRCS) 2011). Most of the basin has B soils, which have low runoff potential when wet (Figure 15). The soil types reported by the SSURGO database might not represent the current soil infiltration/runoff capacity since agriculture and other soil disturbances can significantly change soil characteristics. However, the SSURGO information is the most complete information available for large areas and for more accurate information field surveys would be necessary.

It was assumed that the soil hydrologic capacity did not change between the time of the GLO survey and the present, although this is most likely not the case. In almost two centuries the soil has been modified (e.g. compacted) so much that this is likely have had an effect in its hydrologic capacity. However, there is no data for the soil hydrologic type for the time of GLO and therefore this assumption had to be made.

3.3.4 Curve Number

The CN depends on the soil hydrological group, the cover type, the cover treatment and the hydrologic condition. The soil hydrologic group and cover type were obtained online in the sources described above and entered into ARC-GIS. The cover treatment is a classification for cultivated lands and it was assumed to be straight row crops. The hydrologic condition describes the effects of treatment and cover type on runoff, and it was assumed to be good for all cases.

The CNs assigned to the different cover types can be found in Tables 3 and 4. The composite CN for the basin (assuming AMC II) changed from 57.5 at the time of the GLO survey (Figure 16) to 72.6 on 2001 (Figure 17). The CN for both land covers and for the different AMC can be found in Table 5. Figure 18 shows the different runoff that would be produced under the different land covers using their composite CN. Using the 24-hour and 10-day rainfall depth for the third (northeast) climate district of Iowa (Huff

& Angel 1992) and the CN method, the rainfall and runoff for different return periods under both land covers can be found in Table 6. It is possible to observe that with more intense rainfalls the relative runoff increase (2001 runoff / GLO runoff) decreases, but it is still significant at the 10-day, 100 year return period.

3.3.5 Rainfall

Two rainfall products were used as inputs for the model. The first product is a Hydro-NEXRAD product (15- minute information), developed by Bongchul Seo at the IIHR-Hydroscience and Engineering of the University of Iowa. This product uses the information from the following radars: KDMX (Des Moines, IA), KDVN (Davenport, IA), KARX (La Crosse, WI) and KMPX (Minneapolis, MN). A bias correction of 0.56 was applied to the data obtained based on information from the rain gauge network for Iowa City. This was done because the main purpose of this product was to be applied to the Iowa/Cedar River basins (Figure 9). The second product was the Stage IV product (hourly) from the NCEP (National Center for Environmental Prediction), which uses radar and gauges (multi-sensor) precipitation analysis to produce the data. Figure 19 shows the comparison of the accumulated rainfall (in millimeters) for the period starting on May 29th, 2008 and ending on June 23rd, 2008. The rainfall accumulation obtained with the Hydro-NEXRAD data (200 mm) is lower than the rainfall accumulation obtained with the Stage IV data (270 mm).

3.3.6 Observed discharge

The observed discharge data was obtained online from the USGS at their Instantaneous Data Archives (IDA) (USGS 2010a). A maximum annual discharge of 40,500 cfs (1148 m^3) was published for Elkader for June 10th, 2008 (USGS 2011c). This value and a value of 36,800 cfs (1043 m^3) reported in the USGS streamflow measurements website (USGS 2011b) are the only values available for this day for Elkader. Data from the IDA was ommited for this day for Elkader, given that the daily mean discharge value calculated from this data deviated by more than 10% from the published mean discharge value. The peak discharge observed in the 2008 flood at Eldorado (50,100 cfs), was much larger than the one recorded for Elkader (downstream). This could be explained due to spatial and temporal variability of the rainfall, to areas of overspilling upstream of Elkader, or to data validity. Even though the quality data of the IDA is not completely assured by the USGS staff, this is the only 15-min data available and therefore it was used as the observed data.

The daily mean discharge reported by the USGS was used to calculate the total water volume that went by Eldorado and Elkader between May 29th, 2008 and June 30th, 2008. The volume estimated for Eldorado was 2.99 x 10^8 m^3 and the volume calculated for Elkader was 4 x 10^8 m^3. The trapezoidal method for integration was also used to calculate the volume of water under the hydrograph for Elkader and for Eldorado that were created with IDA data and with the maximum peak flow reported. The water volume obtained for Elkader for the 2008 event was 3.81 x 10^8 m^3 and the volume of water for Eldorado was calculated to be 2.83 x 10^8 m^3. Since the water volumes obtained with the IDA and the published daily data is similar (around 5% difference), the IDA data was used as a valid source of observed data. Even though unusual, the high peak observed at Eldorado was attenuated by the time the peak arrived in Elkader.

To have a much lower peak discharge observed at Elkader than at Eldorado is not common but it is possible. Figure 20 shows the average daily mean discharge at both stations. Points over the diagonal line represent the times that Eldorado has a daily mean discharge higher than Elkader. As expected, the differences in daily mean discharges is larger during large flood events. Since 2001 (when both stations started keeping daily records) most of the time the daily average discharge has been higher at Elkader. Out of the 3,547 daily records available, 3,459 (97.5%) the daily mean average was higher at Elkader than at Eldorado. Most of the time the daily mean descharge at Elkader has been between 100 and 500 cfs higher than the daily mean discharge at Eldorado (Table 7).

However, on June 9th, 2008 Eldorado had a mean discharge that was 13,800 cfs higher than Elkader's mean discharge and on May 22nd, 2004 Eldorado's mean discharge was 5,500 cfs higher than Elkader's mean discharge. This confirms that having a larger peak at Eldorado than at Elkader is rare, but possible.

Figure 13. Representation of Cunha's model's elements

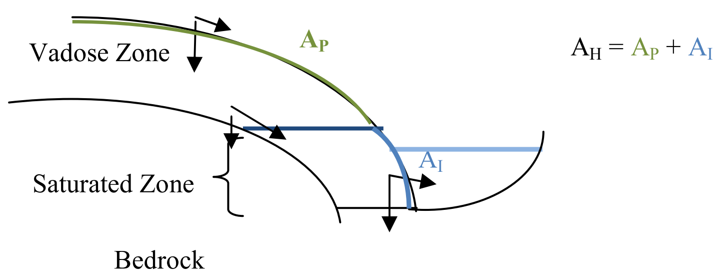

Figure 14. River Network extracted by CUENCAS (orders 3 – 7 are shown)

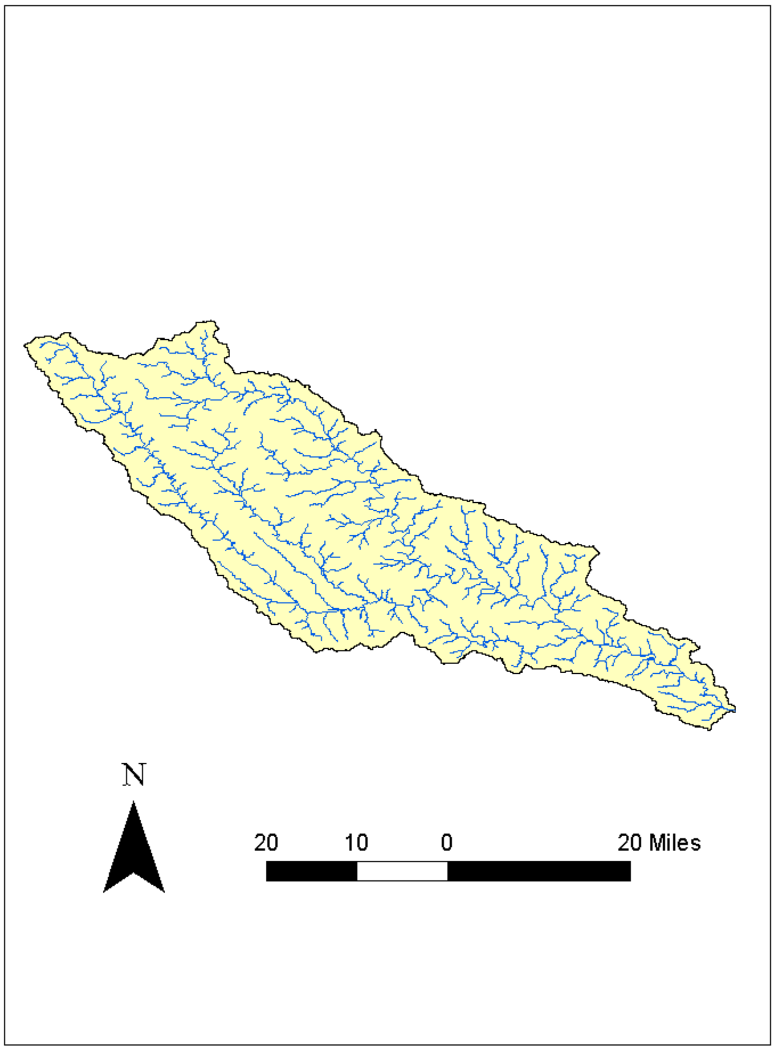

Figure 15. Hydrologic soil types found in the basin

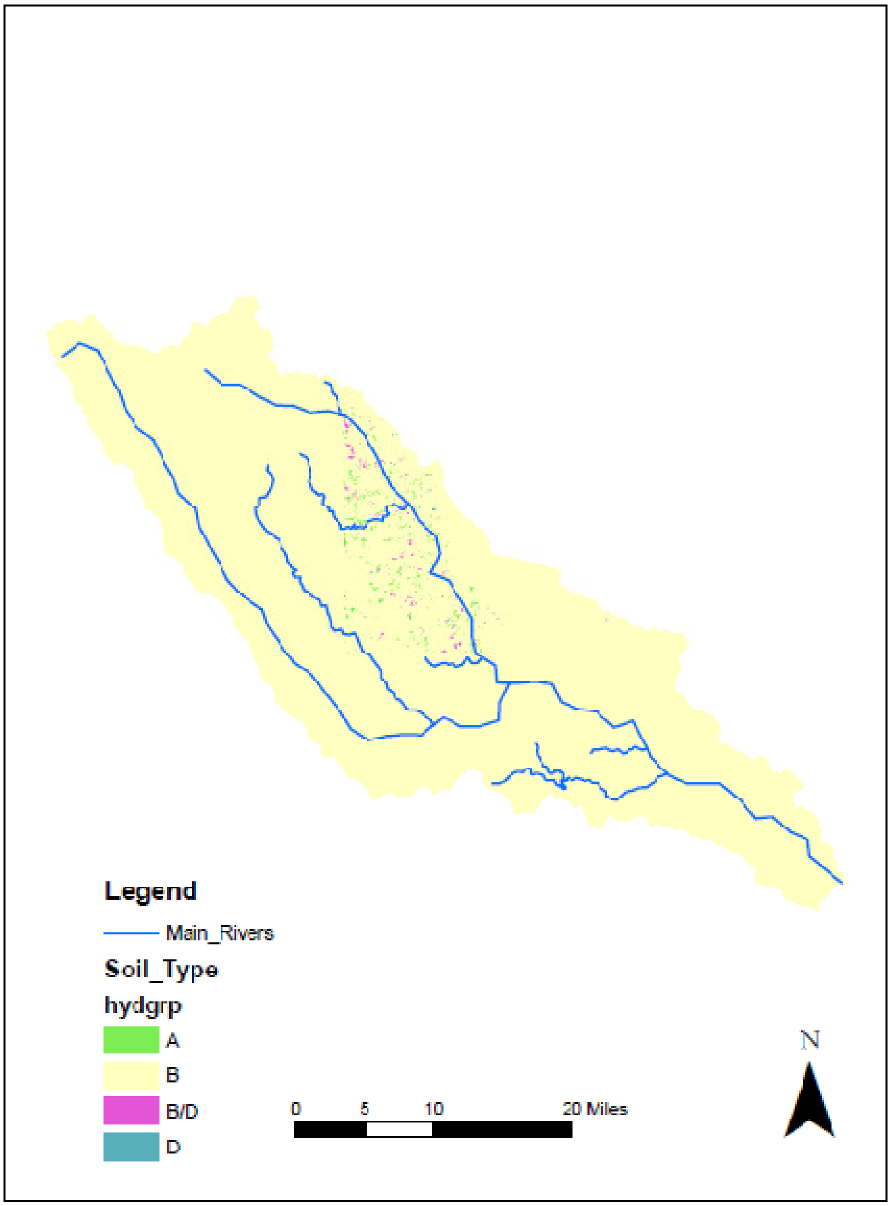

Figure 16. Curve Number for the basin during the GLO Survey (1832-1859)

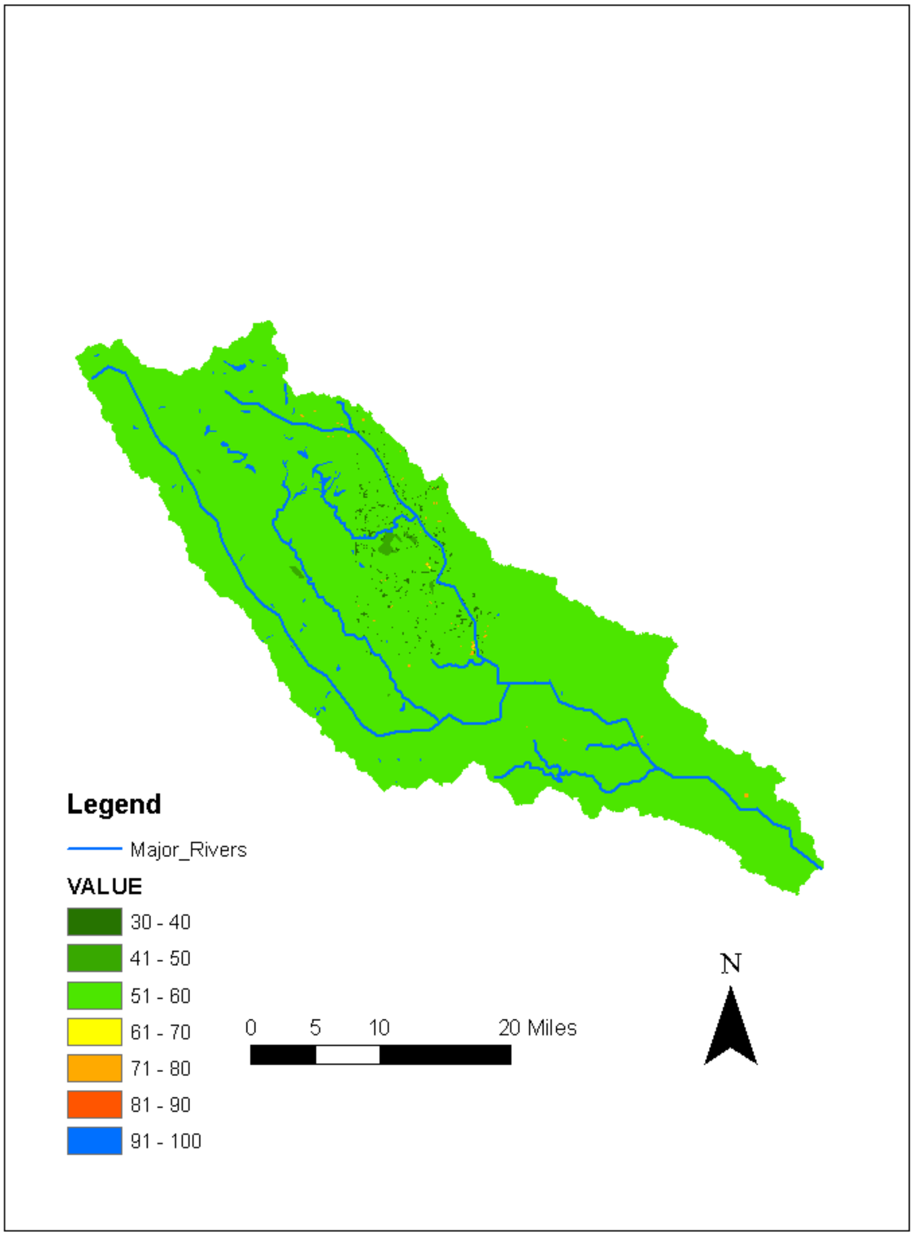

Figure 17. Curve Number for the basin during 2001

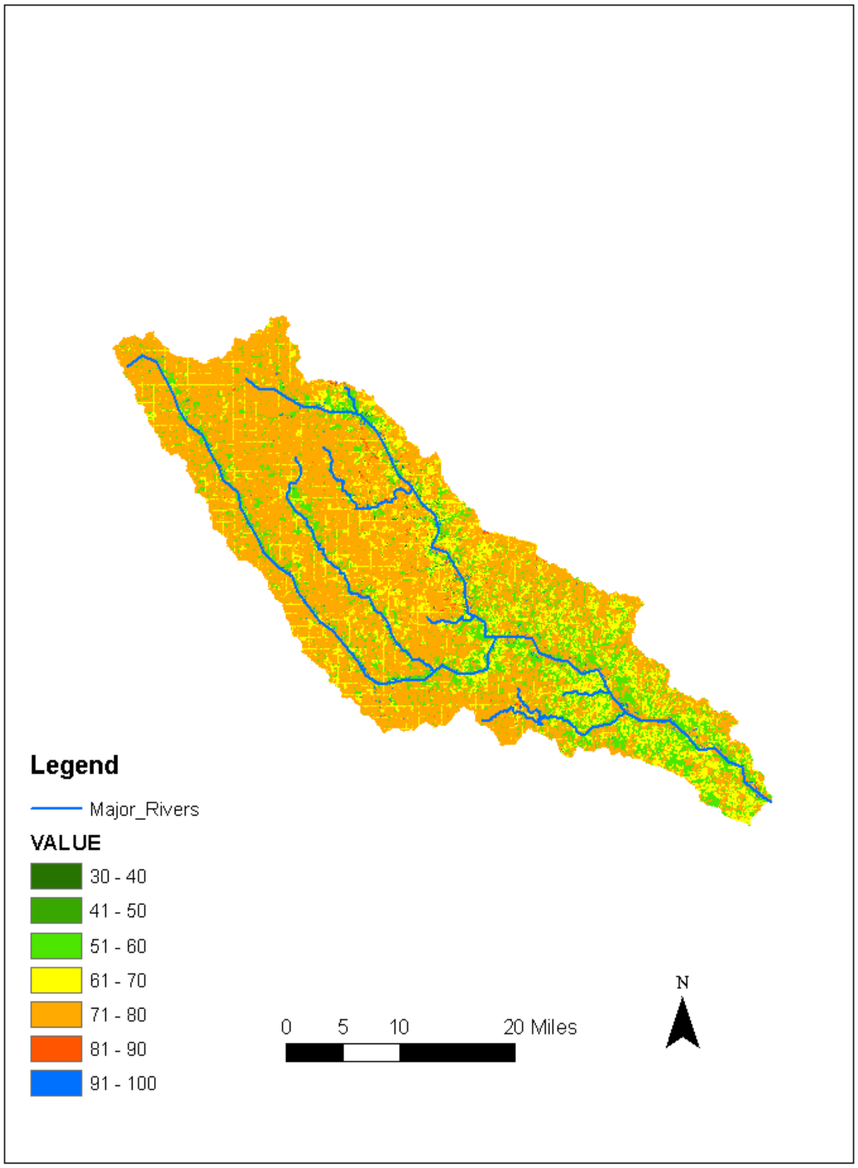

Figure 18. Comparison of rainfall/runoff transformation for the 2001 and GLO land covers using the Curve Number methodology

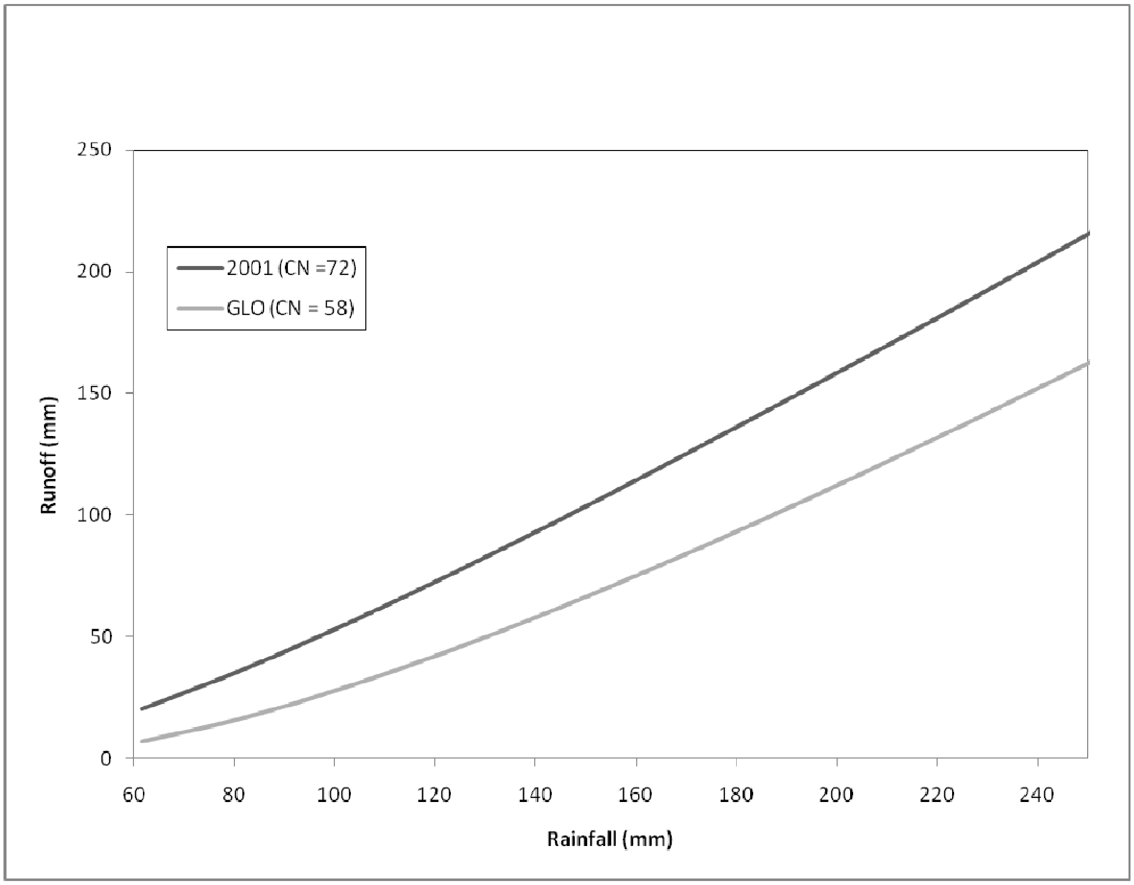

Figure 19. Precipitation accumulation comparison between the Stage IV and the Hydro-NEXRAD rainfall products

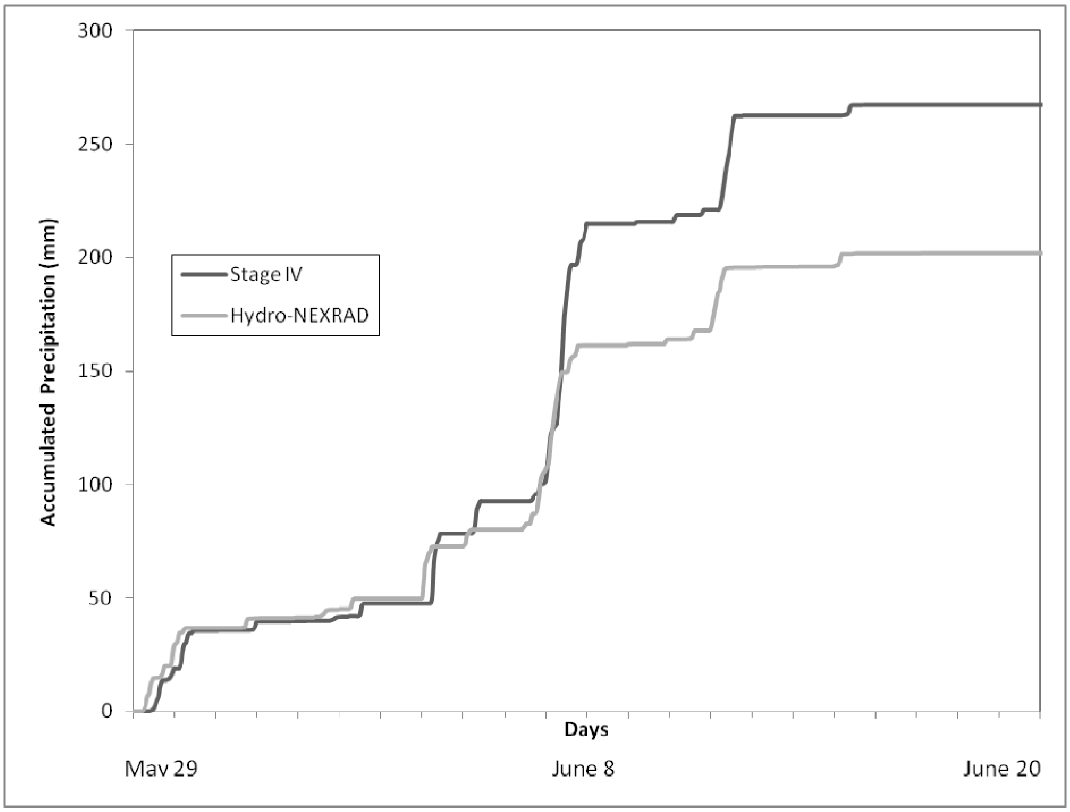

Figure 20. Daily mean discharges at Elkader and Eldorado

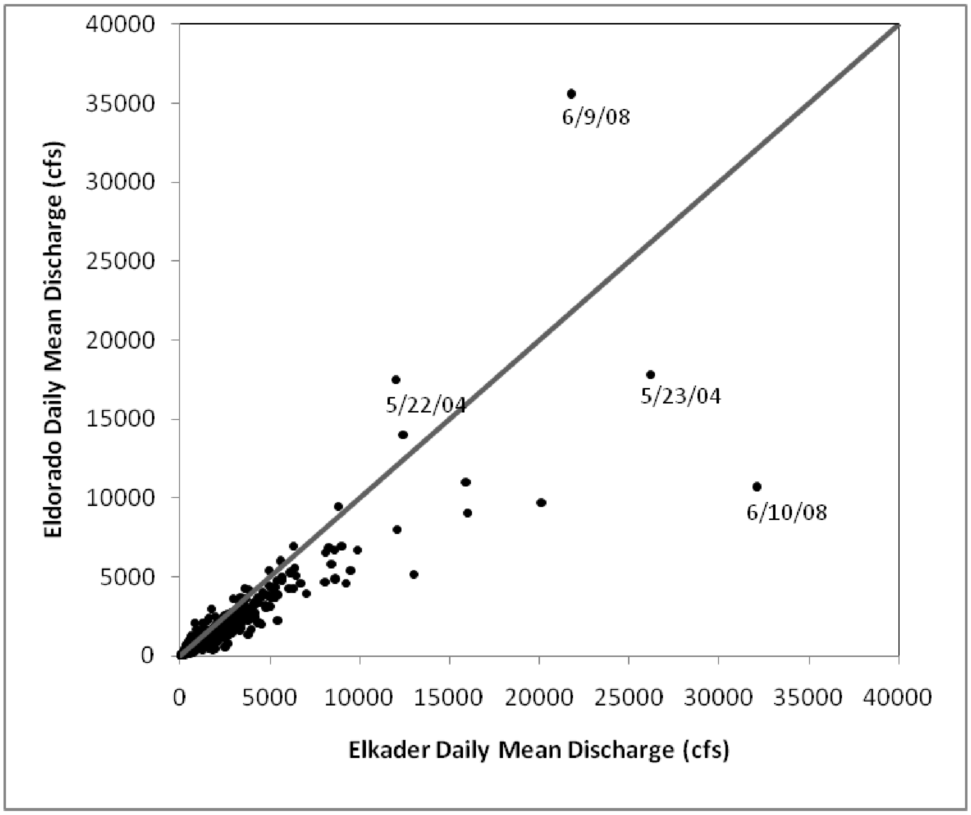

Table 1. Criteria to define the soil Antecedent Moisture Condition (AMC) class

	Total 5-day antecedent rainfall (mm)	
Group	Dormant season	Growing season
I	less than 13	less than 36
II	13-28	36-53
III	more than 28	more than 53

Source: Mishra, S. K., and V. P. Singh. 2003. Soil Conservation Service Curve Number (SCS-CN) Methodology. Kluwer Academic Publishers, Dordrecht, The Netherlands.

Table 2. Codes description and reclassification of GLO codes to 2001 codes

GLO-CODE	GLO-DESCRIPTION	NLCD 2001
PBAY	Bayou	11
PDRA	Drain	11
PLAK	Lake	11
PPON	Pond	11
PRIV	River(border)	11
PSAN	Sandbar	11
PSLU	Slue[sic]	11
PCIT	City	21
PGRO	Grove	41
PISL	Island	41
PRAV	Ravine	41
PROU	Rough	41
PSCA	Scattering trees	41
PTBR	Timber/barrens	41
PTHI	Thicket	41
PTIM	Timber	41
PTSB	Timber/scattering/barrens	41
PTSO	Timber/scattering/openings	41
PWIN	Windfall	41
PBAR	Barrens	52
PBRU	Brush	52
POAK	Oak barrens	52
POPE	Openings	52
PPPT	Part Prairie/part timber	71
PPRA	Prairie	71
PFIE	Field	82
PMAR	Marsh	95
PSMR	Swamp/marsh	95
PSWA	Swamp	95
PWET	Wetland	95

NLCD-2001 CODE	NLCD-2001 DESCRIPTION
11	Open Water
21	Developed, Open Space
22	Developed, Low Intensity
23	Developed, Medium Intensity
24	Developed, High Intensity
31	Barren Land (Rock/Sand/Clay)
41	Deciduous Forest
42	Evergreen Forest
43	Mixed Forest
52	Shrub/Scrub
71	Grassland/Herbaceous
81	Pasture/Hay
82	Cultivated Crops
90	Woody Wetlands
95	Emergent Herbaceous Wetlands

Table 3. Curve numbers assigned to the different cover types of the GLO survey

GLO Code	Cover Description (CN cover)	A	B	C	D	B/D
PBRU	Brush	30	48	65	73	73
PCIT	City (Residential 1/8 acre)	77	85	90	92	92
PFIE	Field	67	78	85	89	89
PGRO	Grove (woods)	30	55	70	77	77
PMAR	Marsh	100	100	100	100	100
PPON	Pond	100	100	100	100	100
PPRA	Prairie	30	58	71	78	78
PROU	Rough (brush)	30	48	65	73	73
PSCA	Scattered Trees (Woods-grass combo)	32	58	72	79	79
PSLU	Slue (slough)	100	100	100	100	100
PSWA	Swamp	100	100	100	100	100
PTBR	Timber/barrens (Woods-grass combo)	32	58	72	79	79
PTHI	Thicket (Woods)	30	55	70	77	77
PTIM	Timber (Woods)	30	55	70	77	77
PTSO	Timber/scattering/oppenings(Woods-grass combo)	32	58	72	79	79
PVIL	Village (Residential 1/2 acre)	54	70	80	85	85

Table 4. Curve assigned to the different numbers cover types found on 2001

2001 Code	Cover Description	A	B	C	D	B/D
11	Open Water	100	100	100	100	100
21	Developed Open Space	39	61	70	80	80
22	Developed Low Intensity	61	75	81	87	87
23	Developed Medium Intensity	77	85	88	92	92
24	Developed High Intensity	89	92	94	95	95
31	Barren Land	77	86	90	94	94
41	Deciduos Forest	32	58	68	79	79
42	Evergreen Forest	32	58	68	79	79
43	Mixed Forest	32	58	68	79	79
52	Shrub	30	48	60	73	73
71	Grassland/Herbaceus	30	58	68	78	78
81	Pastures	39	61	70	80	80
82	Cultivated Crops	67	78	84	89	89
90	Woody Wetland	100	100	100	100	100
95	Emergent Herbaceous Wetland	100	100	100	100	100

Table 5. Curve Numbers for the basin under different Antecedent Moisture Conditions and land covers

	2001	GLO
AMC I	53	38
AMC II	72	58
AMC III	86	76

Source: Mishra, S. K., and V. P. Singh. 2003. Soil Conservation Service Curve Number (SCS-CN) Methodology. Kluwer Academic Publishers, Dordrecht, The Netherlands.

Table 6. 24-hour and 10-day precipitation depth and predicted runoff using the Curve Number method for different return periods for northeast Iowa under two land covers

	24-hour				10 -day			
Return Period	1-year	2-years	10-years	100-years	1-year	2-years	10-years	100-years
Rainfall depth (in)	2.32	2.91	4.31	6.36	4.22	5.04	7.07	10.19
Runoff 2001 (in)	0.42	0.74	1.65	3.25	1.62	2.23	3.89	6.66
Runoff GLO (in)	0.09	0.23	0.78	1.94	0.77	1.19	2.46	4.78
Runoff increase	4.93	3.17	2.11	1.67	2.11	1.87	1.58	1.39

Table 7. Difference in the daily mean discharges between Elkader and Eldorado

Daily mean discharge Elkader - daily mean discharge Eldorado	Frequency
less than -10000	1
from -10000 to -5000	1
from -5000 to -500	12
from -500 to -100	24
from -100 to -50	13
from -50 to 0	37
from 0 to 50	231
from 50 to 100	680
from 100 to 500	2154
from 500 to 5000	389
from 5000 to 10000	3
more than 10000	2

CHAPTER IV: RESULTS

4.1 Model Performance

Several simulations were run to evaluate the performance of Cuencas reproducing the 2008 event at Eldorado and Elkader, to assess its sensitivity to several parameters (rainfall product, stream velocity, runoff coefficient, land cover component) and to determine the parameters values that fit the basin the best. Once the parameters that fit the basin the best were chosen, the model was used to simulate the 2008 event using the land cover found in the basin during the GLO survey (1832-1857) and during 2001.

The performance of the model was assessed by comparing the simulated hydrographs to the observed hydrographs, looking particularly at the timing of the peaks and their shape (width and height). Three quantitative assessments of the goodness of fit of the simulations with the observed hydrographs were calculated to assist in the determination of the best set of parameters. The coefficient of determination (R^2), the Nash-Sutcliffe model efficiency coefficient (Nash coefficient) and the Root Mean Square Error (RSME) can be found in Table 9.

4.1.1 Rainfall product

Since the total amount of precipitation varied significantly between the HydroNEXRAD and Stage IV (NCEP) products (200 mm vs. 270 mm) (Figure 19), the model was run to compare the hydrographs produced with both products. The model was run with a constant velocity of 1 m/s and a runoff coefficient of 1.0 to test the rainfall product.

The HydroNEXRAD product appears to not have enough water to produce the peaks observed at Eldorado (Figure 21). This suggests that the bias correction applied to Iowa City (0.56) is not applicable in the Turkey River Watershed. Therefore, the Stage IV product from NCEP was selected to run the simulations to analyze the 2008 flood.

The changes observed in the hydrographs produced with Cuencas when using the different rainfall products make physical sense since the hydrographs produced with the product with more water produce larger and wider peaks

The accumulated daily and hourly precipitation in the basin (Stage IV product) can be found in Figure 22 and Figure 23, respectively. When plotting the rainfall and discharge at Elkader (Figure 24) it is possible to observe the response of the basin to precipitation. For instance, the small peak produced around June 5th seems to be caused by precipitation that fell really close to the outlet, since there were precipitation events just before the peak. Figure 25 shows the total precipitation observed in the basin on June June 5th. It is possible to observe that a significant event occurred close by the basin's outlet, and that there was precipitation in the entire basin which contributed to the increase in discharge observed on June 6th to June 8th. Table 8 and Figure 22 also show that June 5th had significant precipitation.

The precipitation that fell from the afternoon of June 7th (Figure 26) until the end of June 8th seems to have caused the large peaks observed on June 9th and 10th. It is possible to observe that the entire basin experienced significant rain. The earlier response of the basin is likely caused by rain that fell in the lower part (close by the outlet) of the basin and the peak of June 10th is likely the result of the precipitation that fell in the higher part of the basin.

The last peak observed from June 12th to June 14th was likely caused by the rainfall of June 12th (Table 8). The basin responded quickly to this event because a significant amount of rain fell close to the outlet and the soils were saturated by this point (Figure 27). In summary the response of the basin to rainfall depends on the intensity of rain, but also on the location of this rain- a faster response is expected from rain that fells close to the outlet of the basin, and a slower and more attenuated response is expected from rain that falls in the headwaters.

4.1.2 Stream velocity

The second analysis was done changing the stream velocity. Several simulations were run using constant velocities and nonlinear velocities.

When running simulations with constant velocity, λ_1 and λ_2 are equal to zero and $K = v/l$. To choose an initial constant velocity to run the model, an analysis on the total travel time for water that falls in the basin was performed using ARC-GIS (Figure 28). When using a velocity of 0.75 m/s the water from the most distant link in the basin takes almost 3 days (71 hours) to get to the outlet, which agrees with the value published in the Iowa Flood Information System (IFIS) website of the Iowa Flood Center (IFC 2011). To test the sensitivity of the model to constant velocities, the velocities of 0.75 m/s and of 1 m/s were used for these simulations.

Both velocities (0.75 m/s and 1 m/s) fit the observed data reasonably well (R^2 vary between 0.83 and 0.89). It appears that the constant velocity of 1 m/s produces the main peak (June 10th) around the same time than the observed peak at Eldorado and Elkader, and that the simulations produced using a velocity of 0.75 m/s peak a little later than the observed hydrographs. However the hydrographs produced with a constant velocity of 0.75 m/s have wider peaks that fit the observed data better (Figure 29).

The simulated hygrograph's widths are close to the observed hydrograph width, and the simulated peaks are much larger, but this is expected since a runoff coefficient of one was used. It appears that the stream velocity at Eldorado is larger than the velocity at Elkader, since the peak for the observed discharge hydrograph seems to be to the right of the peak for the simulated hydrograph with velocity equal 1 m/s for Elkader, and to the left of the peak for the simulated hydrograph with the same velocity for Eldorado.

The changes observed in the hydrographs produced with Cuencas when using the different constant velocities make physical sense since the hydrographs produced with the larger velocities peak earlier, and have larger and narrower peaks.

4.1.3 Runoff coefficient

The first order approximation uses a constant runoff coefficient for the rainfall/runoff transformation. The runoff coefficient represents the percentage of rain that is transformed into runoff. The first order approximation assumes that this number does not change in space or time. A low runoff coefficient means that infiltration, evapotranspiration, and other the losses are high, and not much water runs off to the stream network. A high runoff coefficient means that a high percentage of water makes it to the stream network due to low infiltration, evapotranspiration and/or other losses. Four runoff coefficients were used (0.5, 0.6, 0.8 and 1.0) to assess the sensitivity of the model to this parameter and to determine the best fit for the basin.

Figure 30 shows the results of varying the runoff coefficient for Elkader and Eldorado, using a constant velocity of 0.75 m/s. By looking at the figures it appears that a runoff coefficient between 0.6 and 0.8 fits Elkader and a runoff coefficient between 0.8 and 1.0 fits the observed data at Eldorado, when using this velocity. The Nash coefficient and the RSME for these simulations indicate that the best simulations are done when using runoff coefficients of 0.5 and 0.6 These fit parameters also indicate that it is not appropriate to run simulations with a runoff coefficient of 1 (negative Nash coefficients and large RMSEs) (Table 9).

The changes observed in the hydrographs produced with Cuencas when using the different runoff coefficients make physical sense since the hydrographs produced with the larger coefficients have larger and wider peaks, but the timing of the peaks is not affected by these coefficients.

4.1.4 Land cover component

The runoff coefficient is linked to the land cover (through the CN) and to hydrological conditions (through the AMC). Since the land cover varies across the basin (Figure 3) and it has also significantly changed through time (Figure 2 and Figure 4), and since there was enough rain to produce a change in AMC during the 2008 event (according to Table 5, Table 8 and Figure 19), it might help the model performance to assume a variable runoff coefficient to model the 2008 event in the Turkey River basin. The variation in curve numbers and runoff coefficients for the different land covers and AMCs observed in the basin during the 2008 event can be found in Table 5 and Figure 31.

As mentioned before, the first order approximation uses a constant runoff coefficient through space and time. Therefore, to explore the role of land cover in hydrological factors, and specifically in the 2008 floods, Cunha's Model was used to run the following simulations.

A simulation with a constant velocity of 0.75 m/s was run for the 2001 land cover, to observe the effect of including land cover as a parameter in the model. This simulation was compared to a simulation from the first order approximation, using the same constant velocity.

Figure 32 shows the comparison of the model simulations using the first order approximation of Cuencas and Cunha's Model, which takes into account the land cover. These simulations use a constant velocity of 0.75 m/s. The simulation using the first order approximation uses a runoff coefficient of 0.6 for Elkader and 0.8 for Eldorado (those were the runoff coefficients that best fitted the observed data). There are some peaks observed in the simulations before the main peak (around June 10^{th}), that are not in the observed hydrographs. These peaks indicate that the model is not capturing a process that reduces the runoff, like evapotranspiration or infiltration.

When using Cunha's Model the initial peaks that appear around June 1^{st} and June 7^{th} in the simulations with the first order approximation do not exist, matching the observed hydrograph much better. This is the result of including parameters captures the initial soil retention capacity and the delay in the transport of water that exists when the rainfall is infiltrated, and travels underground to the stream. The width of the main peak at Elkader is also better captured with Cunha's model. However, both models overestimate the last peaks produced around June 14th, indicating that none of the models represents the losses of water that exist in the system once the soil is saturated (maybe due to evapotranspiration or to the Kharst geology present in the region). It appears that a parameter in Cunha's Model needs to be adjusted, since the observed hydrograph returns to base level before the simulated hydrograph with Cunha's Model.

A set of simulations using nonlinear velocities was also run. The parameters were $v_o = 0.21$ m/s, $\lambda_1 = 0.15$ and $\lambda_2 = 0.05$, and came from data from USGS stations in Iowa (excluding urban gauges) (Mantilla 2011).

The hydrographs resulting from using Cunha's Model and constant velocity and nonlinear velocity are similar (Figure 33), although for Elkader the nonlinear velocity fits the observed data a little better than the constant velocity (mostly around the main peak). The R^2, Nash coefficient and RMSE for these runs show that for Eldorado the constant velocity actually fits the observed data better, and the non linear velocity fits the observed data better at Elkader (Table 9).

4.2 Land use change effects on flooding

The last run was using the parameters that fit the best the observed data and Cunha's Model to simulate the discharge produced by the 2008 rainfall and the GLO land cover, and compare this discharge to the discharge simulated with the 2008 rainfall and the 2001 land cover.

The simulation that fits better the observed data at Elkader (which is the outlet that defines the basin) appears to be obtained using Cunha's model and nonlinear velocity using $v_o = 0.21$, $\lambda_1 = 0.15$, $\lambda_2 = 0.05$. The R^2s also indicate this is the case, and the Nash coefficient and RSME for this simulation show a good fit to the observed data (Table 9). Therefore these parameters were used to obtain a hydrograph using the rainfall for 2008 and the GLO land cover. This exercise gives a light into the effects that land cover change in this basing could have had in its hydrology. However, since there is no available data of rainfall events and the hydrographs produced during the GLO time, there is no way to validate these results. There are many factors that the models used (first order approximation and Cunha's Model) do not look at that can be important in the flood producing processes. Assuming that Cunha's model captures the main processes that produce floods, the flood produced during the GLO time would have been significantly lower (peak discharge simulated for GLO for Elkader was 699 m^3/s, almost half of 2001 simulated discharges(1300 m^3/s)) than the one observed during 2008 at Elkader and Eldorado (Figure 34). The effect of land cover in the discharges are lower in the peaks produced around June 14th, maybe due to saturation of the land, which reduces the infiltration capacity of all types of land cover, or maybe due to the lack of the Cunha's Model to capture water losses that happen once the soil is saturated.

Figure 21. Hydrographs for Eldorado (top) and Elkader (bottom) using the HydroNEXRAD and the Stage IV rainfall products (Runoff Coefficient = 1, Constant velocity = 1 m/s)

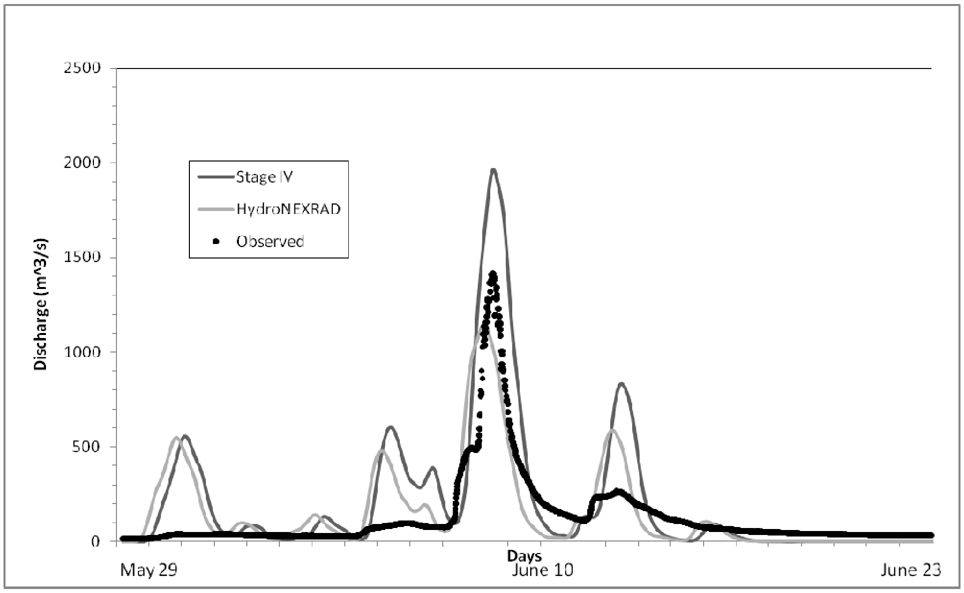

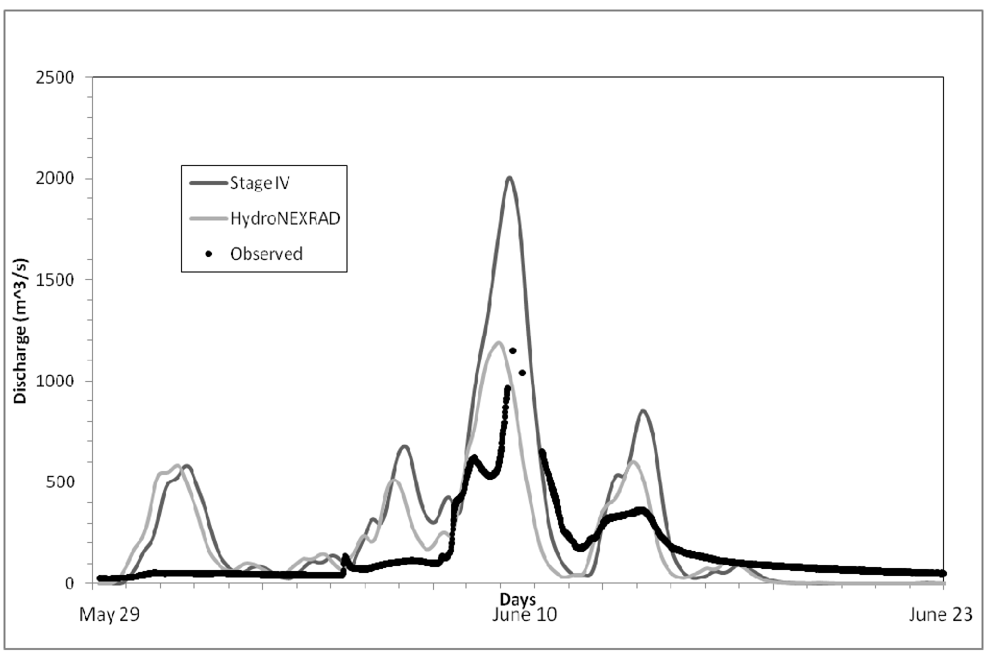

Figure 22. Daily Stage IV precipitation

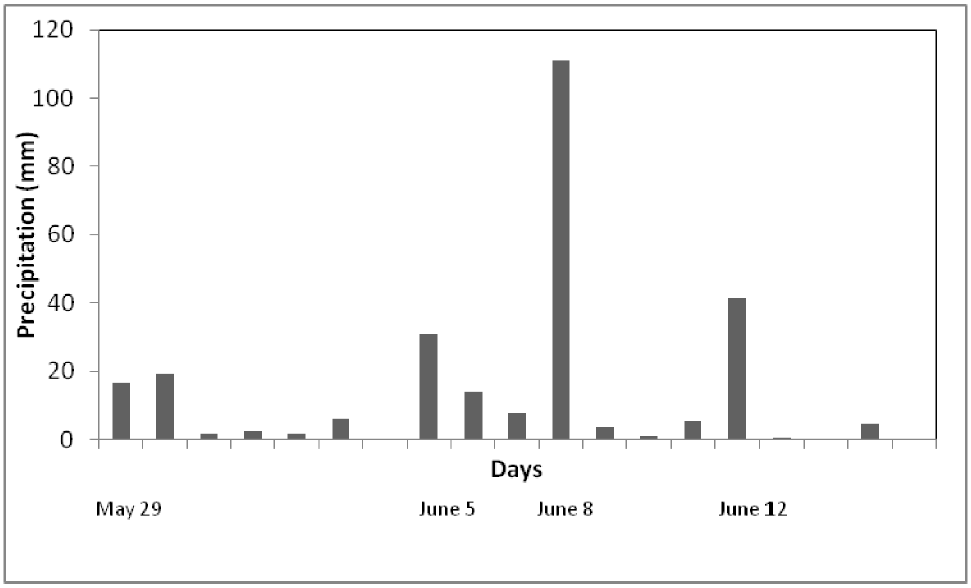

Figure 23. Hourly Stage IV precipitation

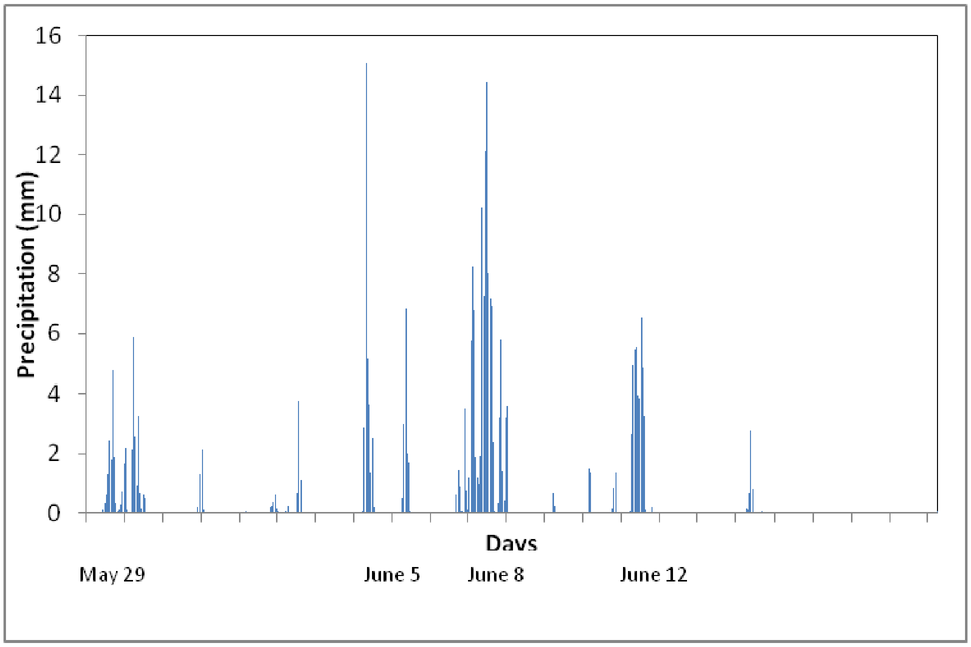

Figure 24. Precipitation and observed discharge at Elkader

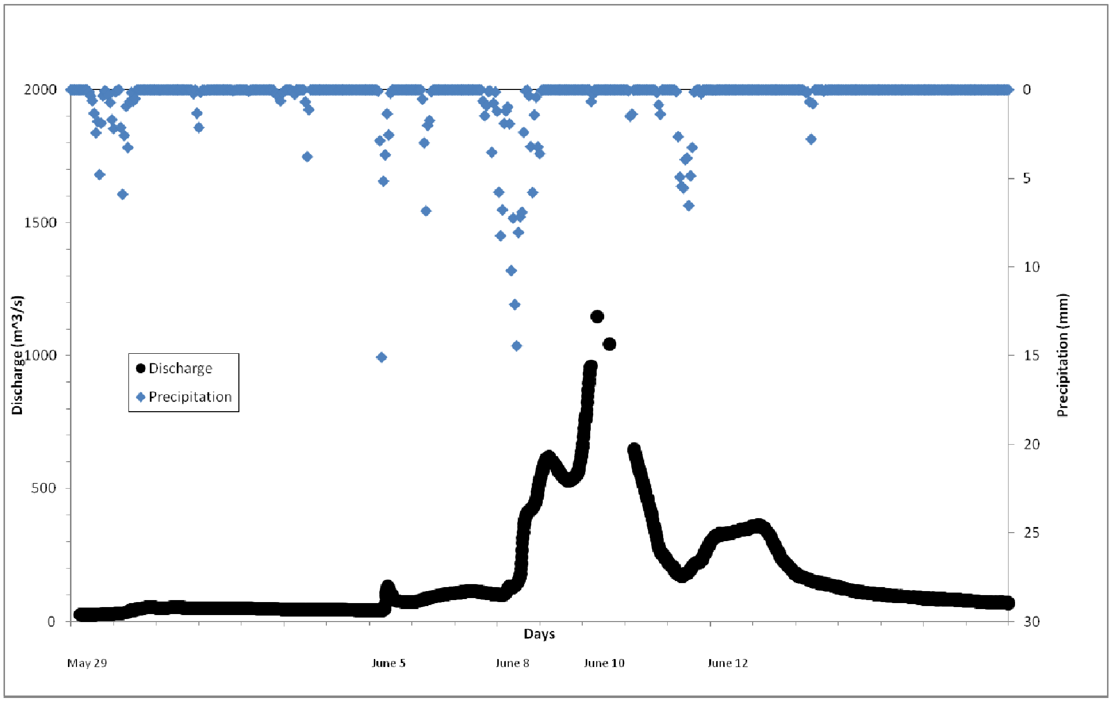

Figure 25. Total precipitation observed during June 5th, 2008

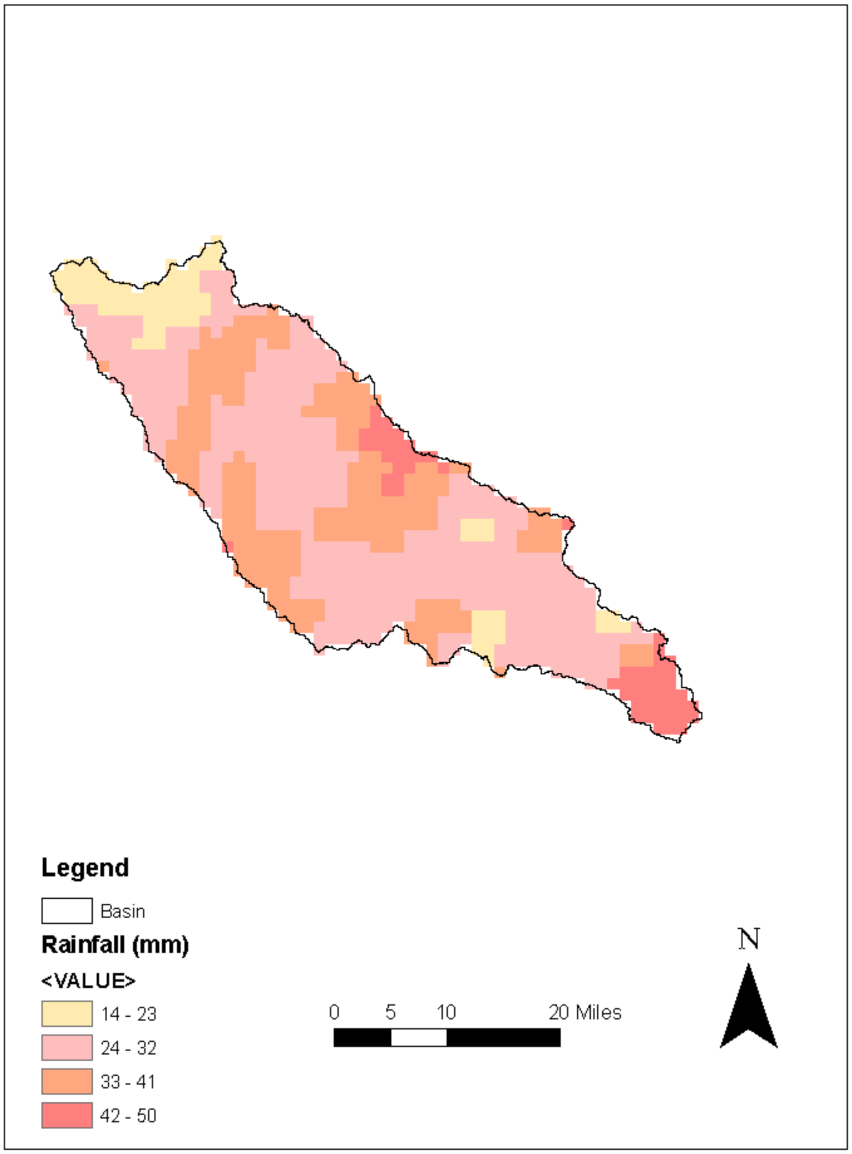

Figure 26. Total precipitation observed on June 7th and June 8th, 2008

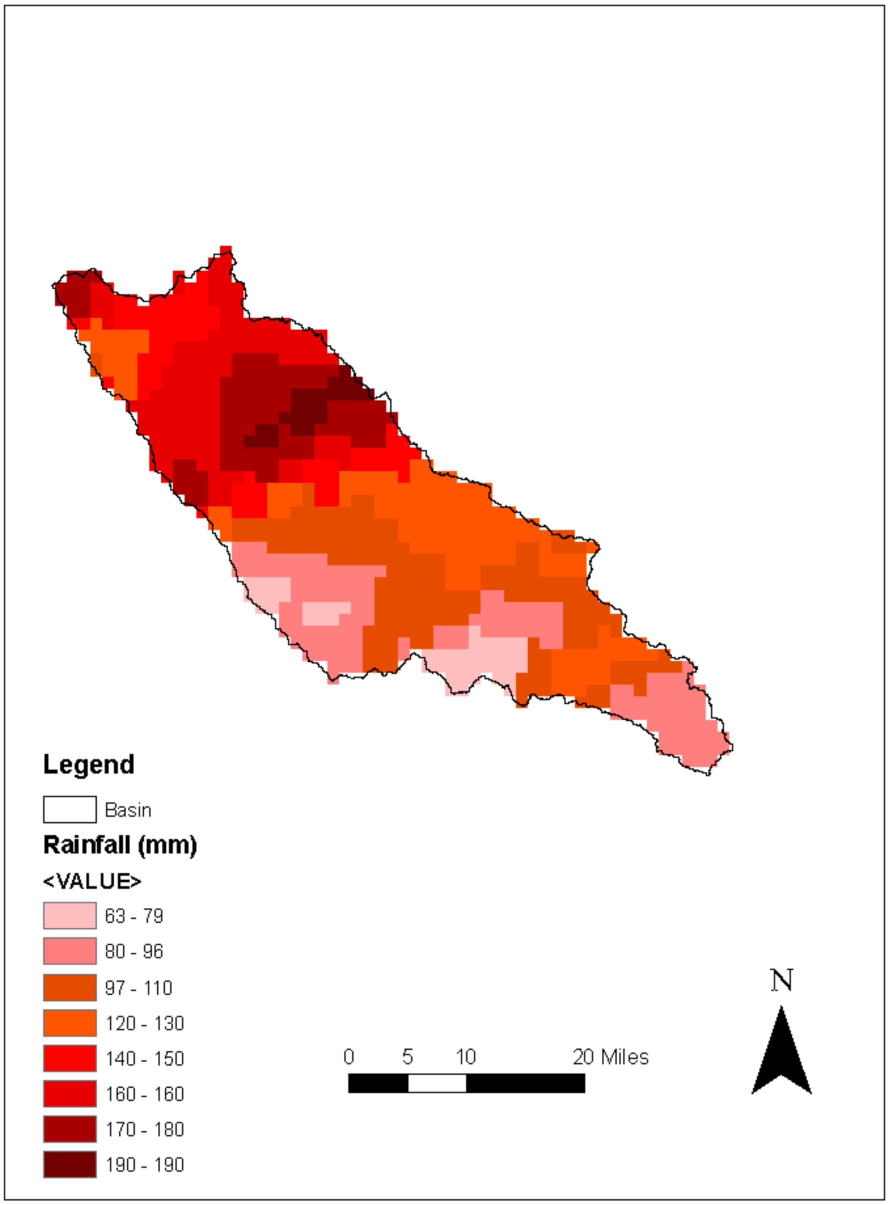

Figure 27. Total precipitation observed on June 12th, 2008

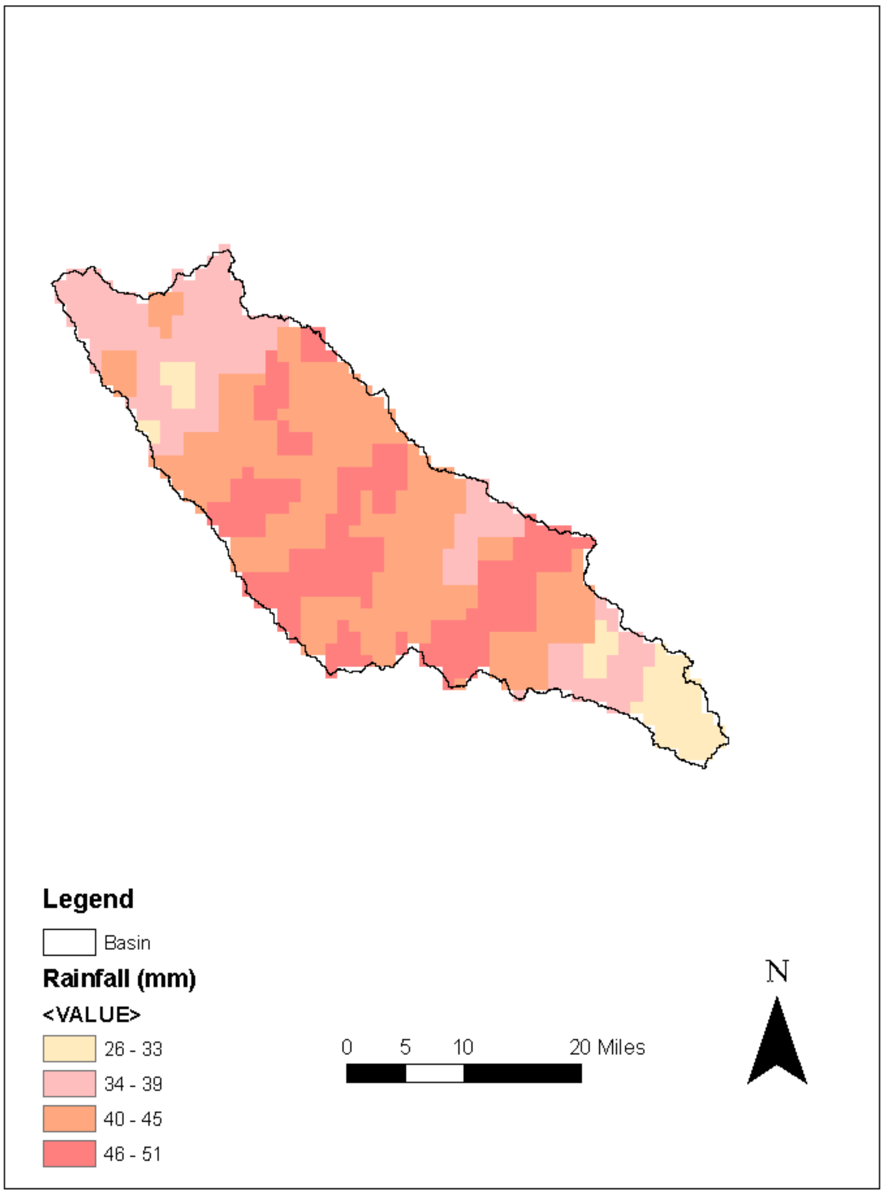

Figure 28. Water travel time using a constant velocity of 0.75 m/s

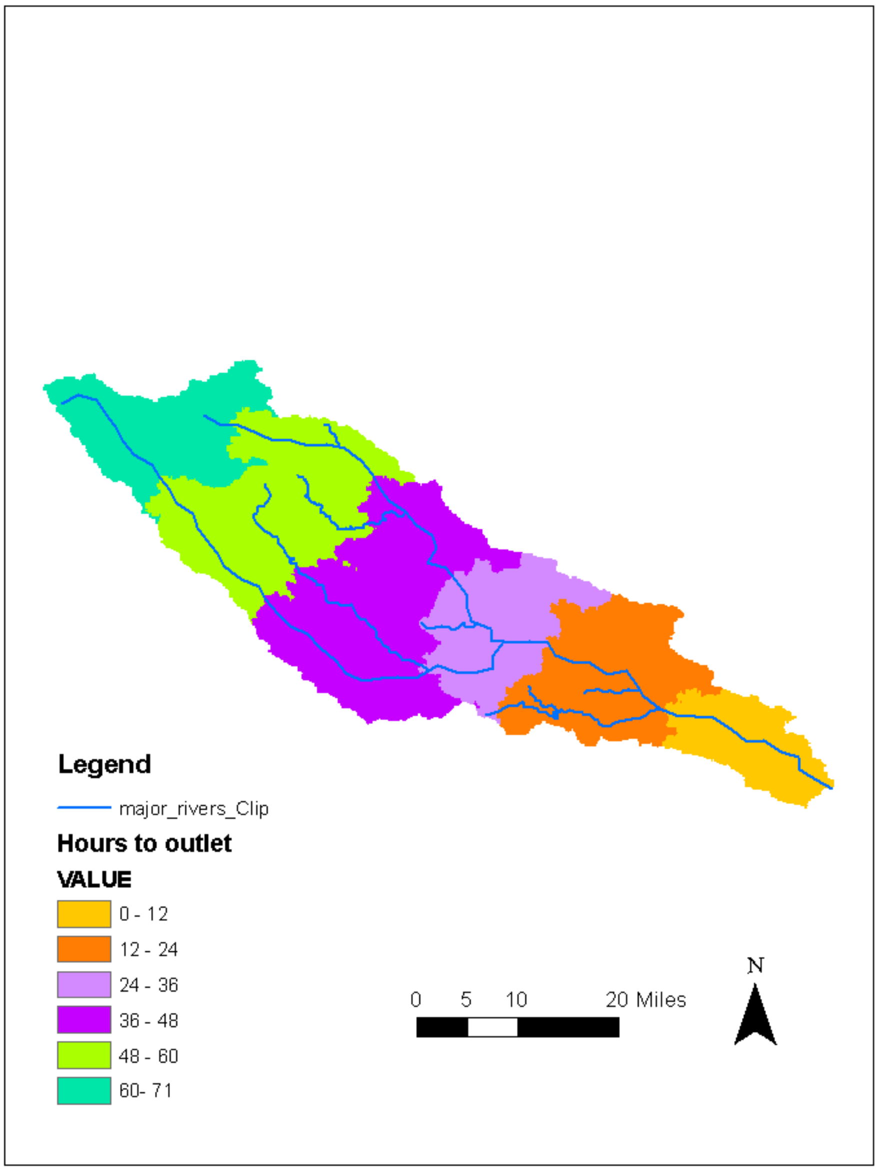

Figure 29. Hydrographs for Eldorado (top) and Elkader (bottom) using different constant velocities (Runoff coefficient = 1)

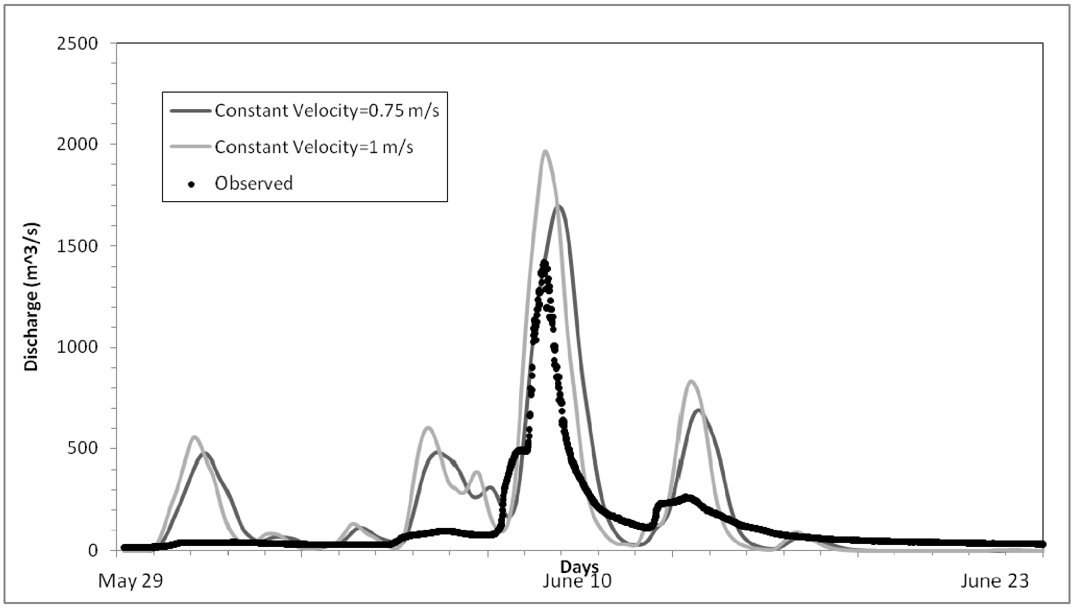

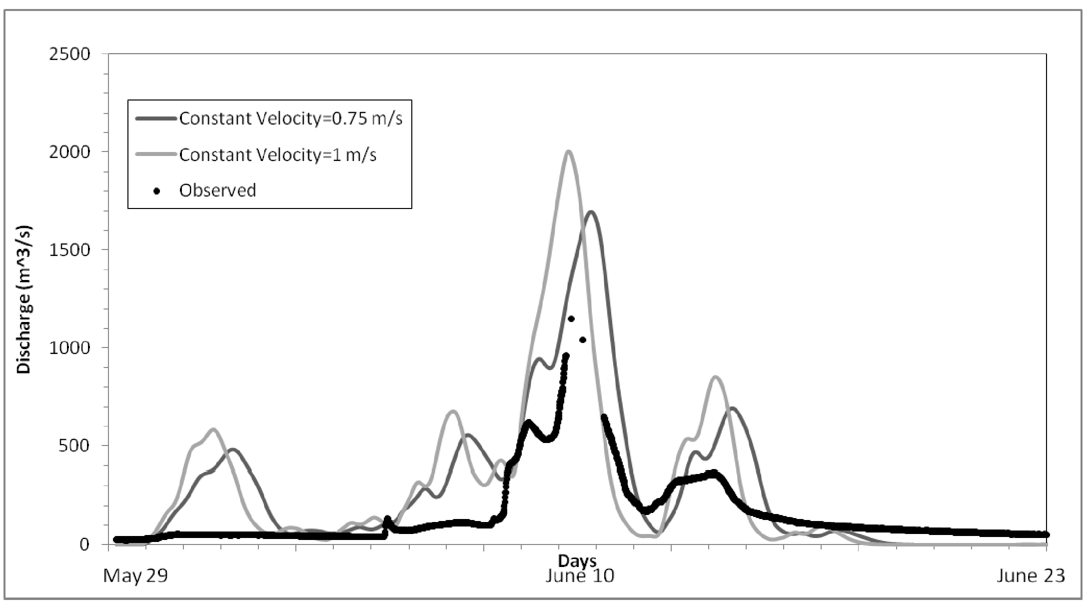

Figure 30. Hydrographs for Eldorado(top) and Elkader (bottom) using a constant velocity of 0.75 m/s and different runoff coefficients (RC)

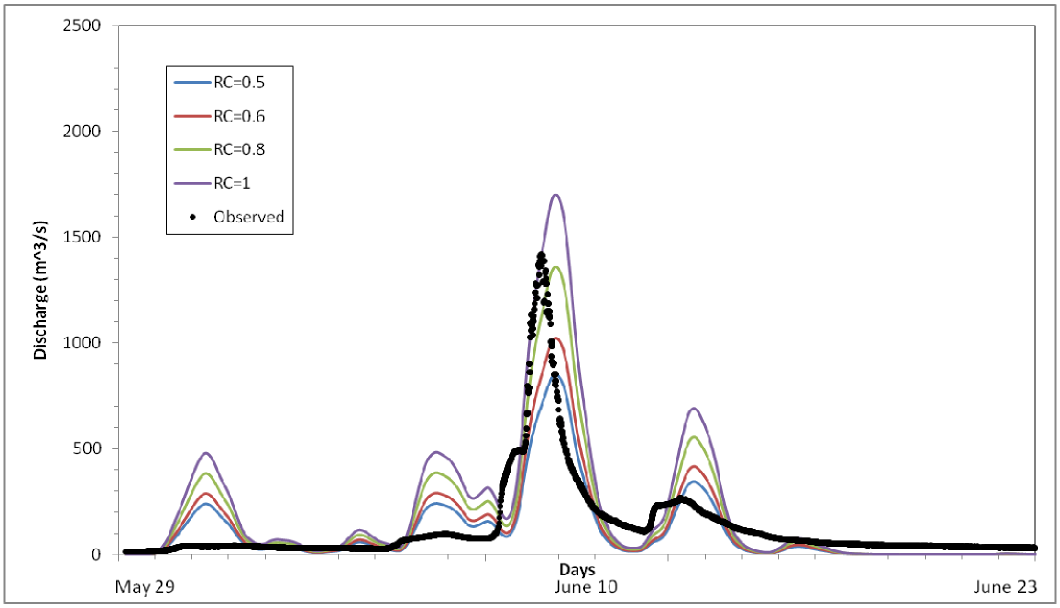

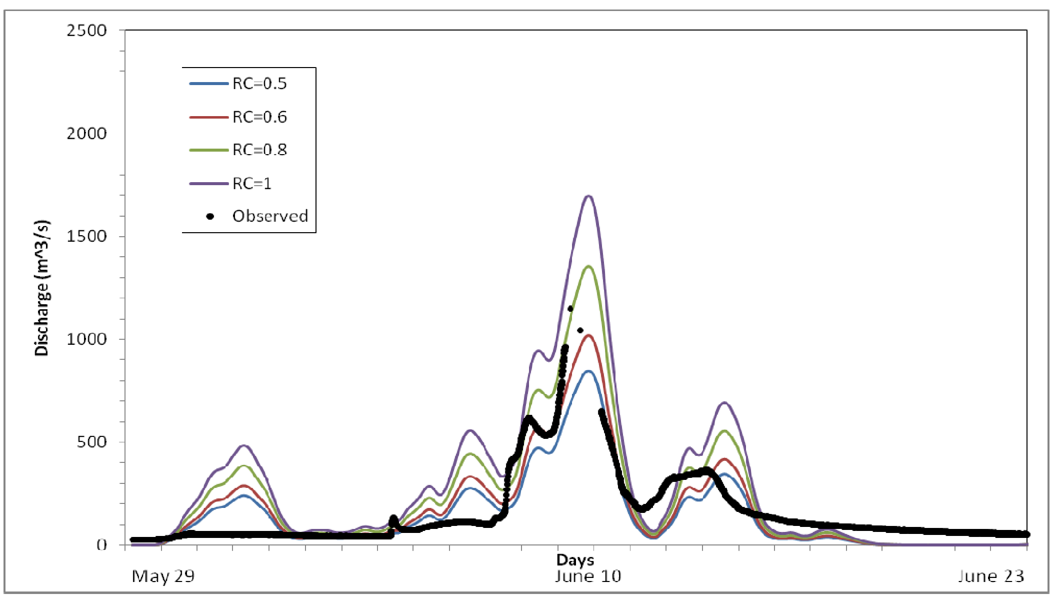

Figure 31. Runoff coefficients for the different land covers and Antecedent Soil Moisture Conditions

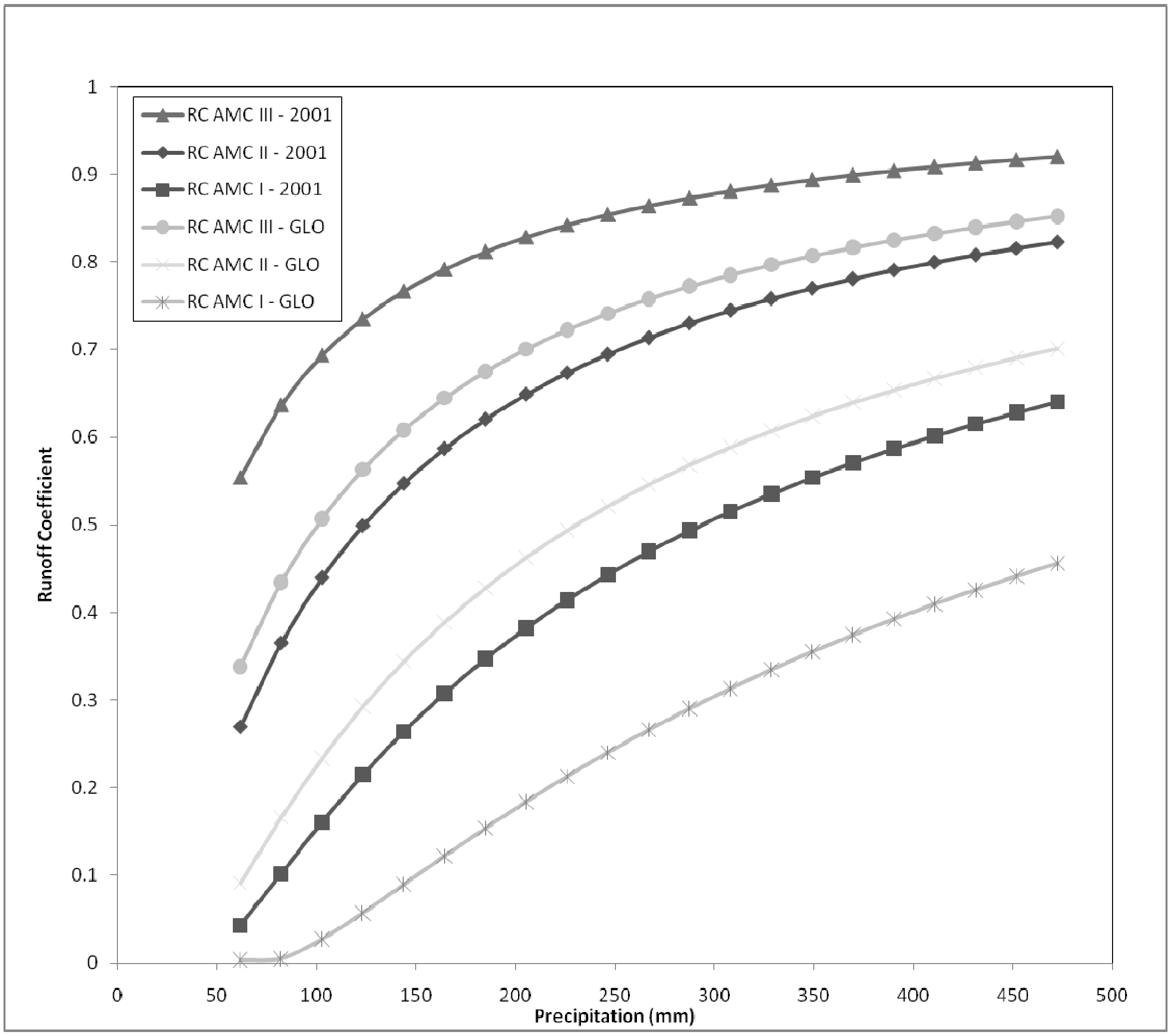

Figure 32. Hydrographs for Eldorado (top) and Elkader (bottom) using Cunha's Model and the First approximation

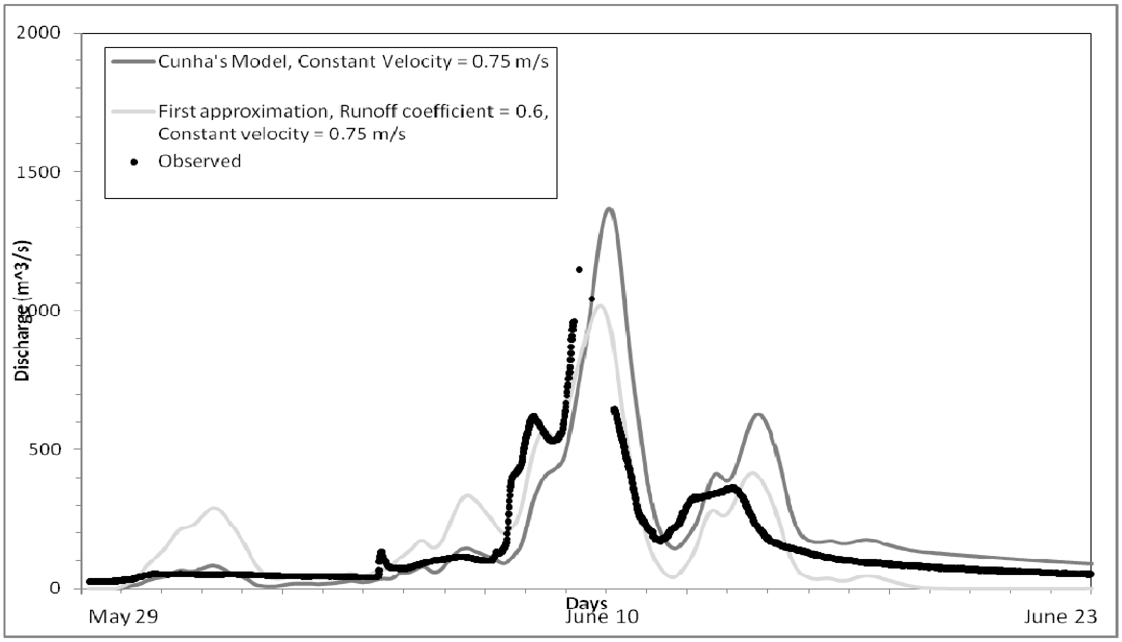

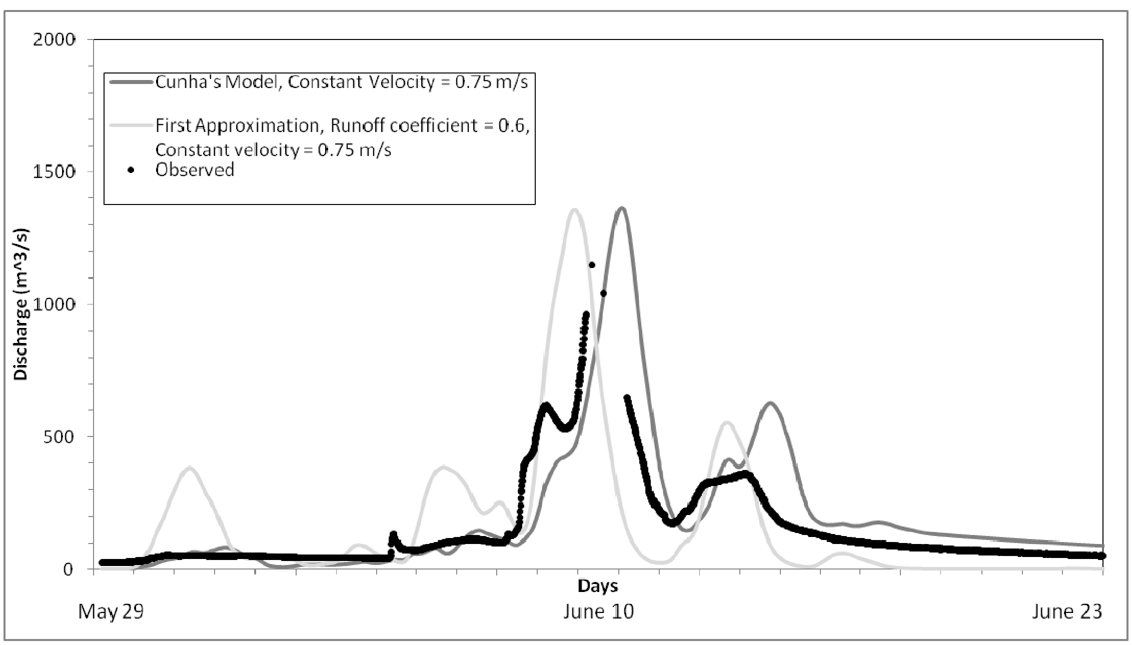

Figure 33. Hydrographs for Eldorado (top) and Elkader (bottom) using Cunha's Model and linear and non linear velocities

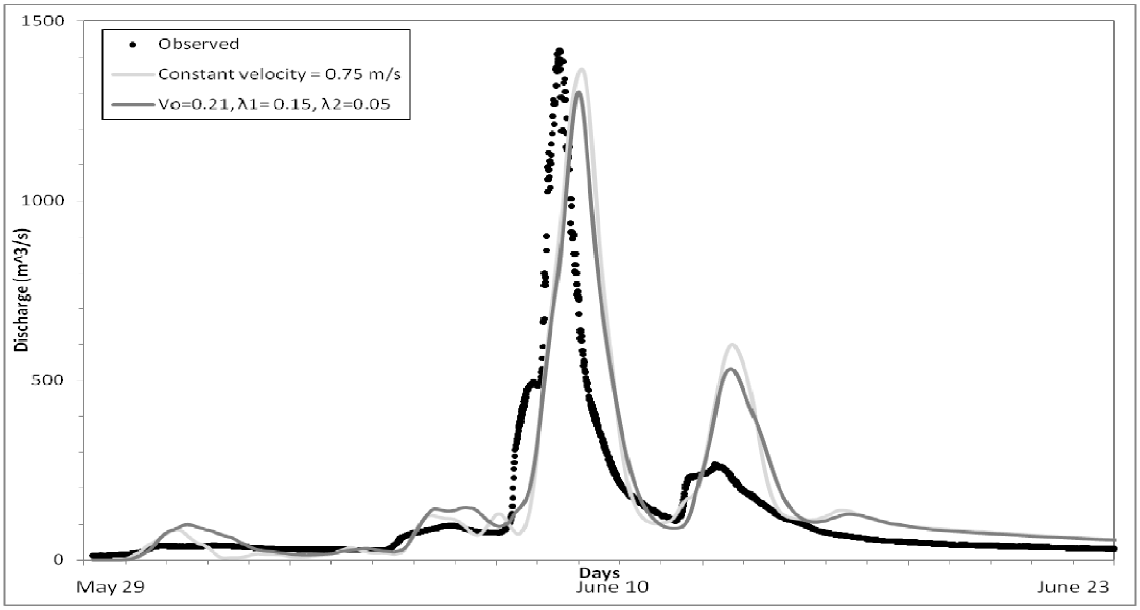

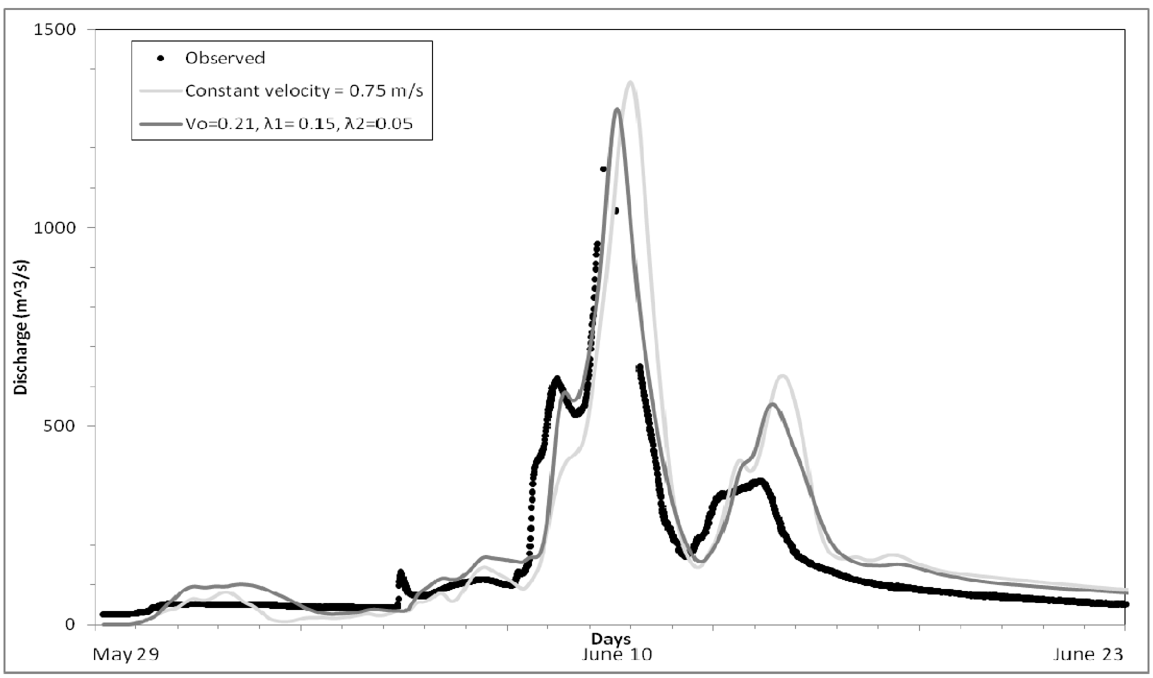

Figure 34. Hydrographs for Eldorado (top) and Elkader (bottom) using Cunha's Model, non linear velocity ($V_o = 0.21$, $\lambda_1 = 0.15$, $\lambda_2 = 0.05$) and two land covers (GLO and 2001)

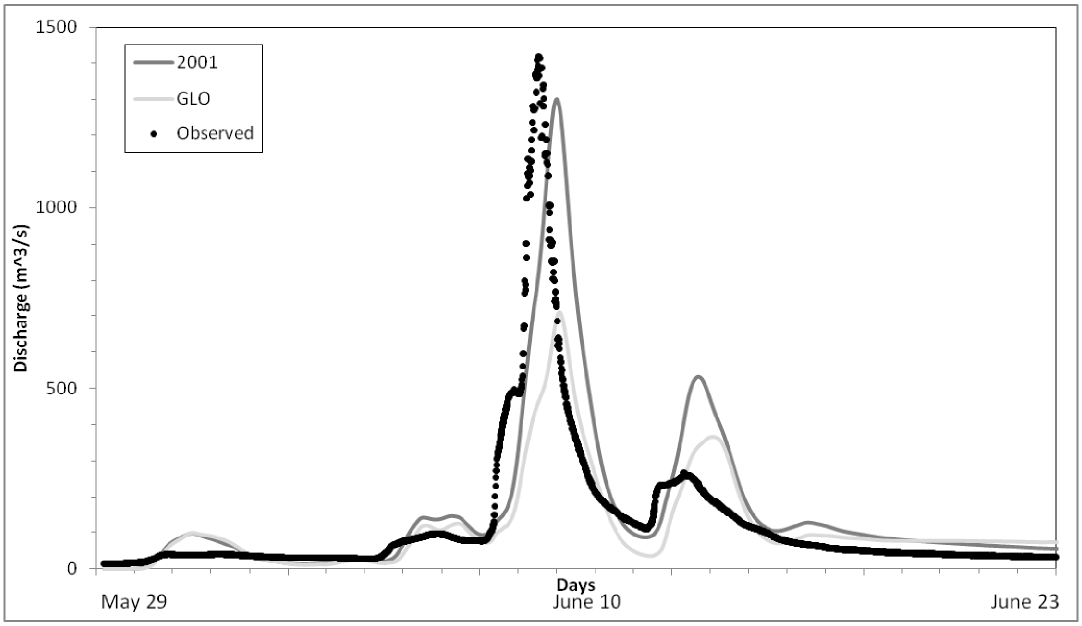

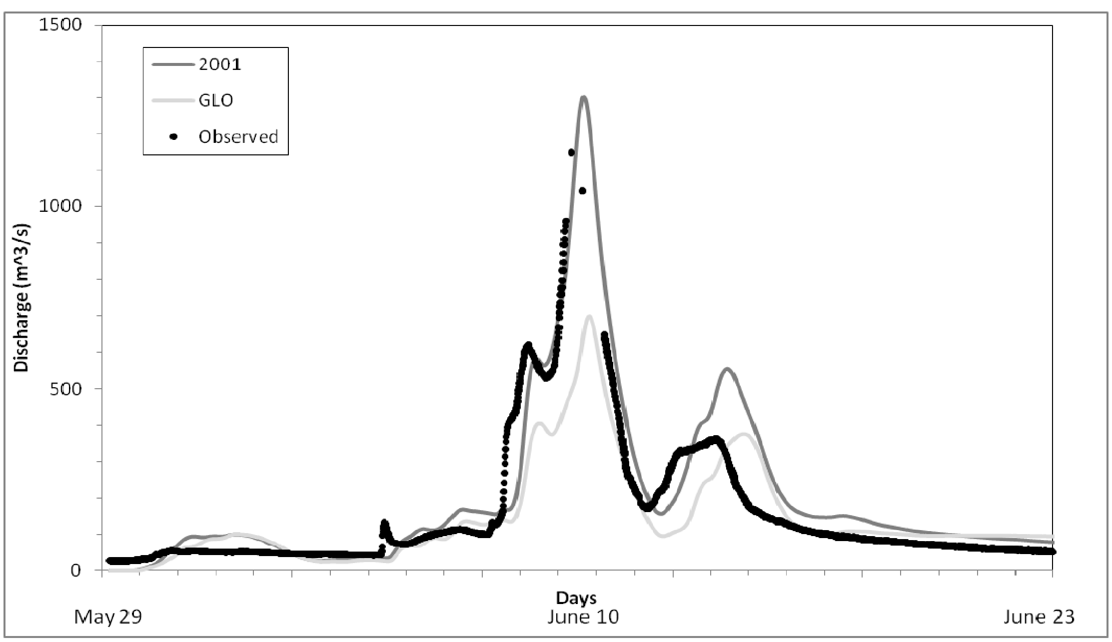

Table 8. Accumulated daily precipitation in the basin

Date	Precipitation (mm)
29-May	16.53
30-May	19.12
31-May	1.56
1-Jun	2.41
2-Jun	1.8
3-Jun	6.02
4-Jun	0
5-Jun	30.93
6-Jun	14.19
7-Jun	7.58
8-Jun	110.94
9-Jun	3.64
10-Jun	0.92
11-Jun	5.34
12-Jun	41.45
13-Jun	0.04
14-Jun	0
15-Jun	4.68
16-Jun	0
17-Jun	0
18-Jun	0
19-Jun	0

Table 9. Goodness of fit parameters for the simulations run

USGS Station	land Cover	Velocity Type	Velocity Parameters	Runoff Coefficient	R^2	Nash	RSME
Eldorado	2001	Constant Velocity	0.75 m/s	0.5	0.84	0.69	119.64
Eldorado	2001	Constant Velocity	0.75 m/s	0.6	0.84	0.69	120.85
Eldorado	2001	Constant Velocity	0.75 m/s	0.8	0.84	0.45	159.29
Eldorado	2001	Constant Velocity	0.75 m/s	1	0.84	-0.07	223.03
Eldorado	2001	Constant Velocity	1 m/s	0.5	0.89	0.78	101.82
Eldorado	2001	Constant Velocity	1 m/s	0.6	0.89	0.76	106.17
Eldorado	2001	Constant Velocity	1 m/s	0.8	0.89	0.47	157.10
Eldorado	2001	Constant Velocity	1 m/s	1	0.89	-0.15	231.41
Eldorado	2001	Constant Velocity	0.75 m/s	Cunha's Model	0.86	0.62	132.17
Eldorado	2001	Non linear Velocity	Vo=0.21 m/s, λ1= 0.15, λ2=0.05	Cunha's Model	0.84	0.61	134.90

USGS Station	land Cover	Velocity Type	Velocity Parameters	Runoff Coefficient	R^2	Nash	RSME
Elkader	2001	Constant Velocity	0.75 m/s	0.5	0.89	0.77	95.86
Elkader	2001	Constant Velocity	0.75 m/s	0.6	0.89	0.73	103.14
Elkader	2001	Constant Velocity	0.75 m/s	0.8	0.89	0.33	164.47
Elkader	2001	Constant Velocity	0.75 m/s	1	0.89	-0.53	247.87
Elkader	2001	Constant Velocity	1 m/s	0.5	0.83	0.62	122.72
Elkader	2001	Constant Velocity	1 m/s	0.6	0.83	0.51	140.78
Elkader	2001	Constant Velocity	1 m/s	0.8	0.83	-0.12	212.03
Elkader	2001	Constant Velocity	1 m/s	1	0.83	-1.27	301.92
Elkader	2001	Constant Velocity	0.75 m/s	Cunha's Model	0.91	0.67	115.66
Elkader	2001	Non linear Velocity	Vo=0.21 m/s, λ1= 0.15, λ2=0.05	Cunha's Model	0.94	0.76	98.74

CHAPTER V: DISCUSSION

5.1 Performance of Cuencas modeling the 2008 flood event

The first order approximation with constant velocity (simplest model formulation) captured relatively well the hydrograph timing for the main peak (around June 10th) for the 2008 event. However, Cunha's Model produced better results before June 10th, suggesting that this model modification captures the main losses of rainfall before runoff is produced. None of the models were able to reproduce the last peak (around June 14th), very well since they produced larger peaks and at a later time than the observed peaks. This indicates that both models lack of a water loss mechanism once runoff has started and the land is saturated (maybe evaporation or deep aquifer infiltration). The most complex simulation (Cunha's Model with nonlinear velocity) produced the results that were the closest to the observed discharges, and was the best in reproducing the timing and shape of the peak flow.

Even though the constant velocity and no land cover is the simplest scenario and requires less resources (computational time, and data to feed the model), Cunha's Model has better physical foundations and captures the width, peak, and timing of the peaks better. This difference in performance seems to be more obvious before the land is saturated, since after the main peak of June 10th both models performed similar.

An advantage of using Cuencas over other more complex physically-based models is that most of the inputs required can be obtained with remote sense information or with field information gathered by government agencies and readily available online. Another advantage of using cuencas is that it can produce results for short time steps. In this case a 15-minute time step was used. Figure 35 shows a comparison of the 2004 hydrograph for Elkader produced when using a 30-min time step versus the hydrograph produced when using a mean daily value. As this figures shows, using a 30-min time step results in better detail of what happen in the event, mostly around the peak. Since the 15-

min discharge data was not available for June 10th, 2008 for Elkader, only two discharge values (one for the estimated peak value, and one for a measured value) were used for that day. Given that the peak of the 2008 event occurred that day, the observed hydrograph that was used in this project might be different from what really happened, as a lot of detail is lost when using daily time steps (Figure 35).

Cuencas (first order approximation and Cunha's Model) was able to reproduce the peak flow for the 2008 event with relatively low inputs, and therefore may be used as an exploratory tool when looking at peak flows.

Given that the objective of the Iowa Flood Center is to develop a model tool that can be used to produce fast and reliable results for large scales (state wide), it is important to keep the model as simple as possible to reduce computer resources and modeling time. The running time of these project's simulations was around 2 hours, which is a reasonable time for such a large watershed area (900 mi^2 or 2300 km^2). This is an indication that Cuencas can be used to predict floods at a real time and at large scales.

5.2 Role of land cover change in the 2008 flood event

Wehmeyer et al. (2011) found that the CN for the Turkey River Watershed was 59.3 by the time of the General Land Office (GLO) survey (1832 to 1859) and 75 by the time of the Illustrated Atlas of the State of Iowa (1875). These numbers differ a little from the numbers found in this study, but the studies have slightly different area and used different CNs for the different categories. The fact that the CN for the basin had increased to the middle seventies by 1875, show that the main land cover transformation in the basin happened over 135 years ago. Therefore, even if some of the vegetation of the basin is restored, it may take a long time to restore the hydrologic properties of the soil, after so many years of agricultural use.

Assuming that Cunha's Model captures the main processes generating floods in the Turkey River Basin, the drastic land cover change of Iowa had a significant effect on the flood of 2008 at Elkader. The peak flows produced when using the 2001 land cover are 1.9 times the peak flows produced when using the land cover before this transformation happened (699 m^3/s vs. 1300 m^3/s). If the USGS current rating curve for Elkader is used (Figure 36), the predicted discharge with the 2001 land cover would have a flow depth of 29 ft (there is no rating curve for this value, since it is higher than the maximum observed value), and the predicted discharge for the GLO land cover would have a flow depth around 22.5 ft. This reduction in flow depth could save a significant upland area from being flooded. Using an estimated total rainfall for the period from June 7^{th} to June 9^{th} of 122 mm (Table 8), a Curve Number of 72 for the 2001 land cover and of 58 for the GLO land cover, the total runoff predicted with the CN methodology under the 2001 land cover is 52 mm and under the GLO land cover is 27 mm. This means that the runoff under the 2001 land cover is 1.9 times higher than the runoff produced under the GLO land cover, which is the same rate observed with the predicted peak discharges of June 10^{th}.

The effects of land cover in the hydrology of the basin can be also observed when comparing the runoff coefficients and stream velocities for Eldorado and Elkader. The basin at Eldorado encompasses the region of the watershed that is more agricultural (and less steep), and therefore, the different land cover might be the reason why Eldorado seems to have larger velocities and runoff coefficients.

The results found in this thesis are applicable only to the storm characteristics of 2008 at Elkader and Eldorado, but could be really different when using other storms, or in other areas. To explore the spatial variability of flooding, the relative peak reduction (peak simulated for 2001/ peak simulated for GLO) was calculated for 145 subwatersheds in the basin (Figure 37). In 38.6% of these subwatersheds, the peak flow reduction was between 1 and 1.5 times; in 55.9% of these subwatersheds, the peak flow reduction was between 1.5 and 2 times, and in 5.5% of these subwatersheds the peak reduction was higher than 2 times. In average, there was a peak reduction of 1.6 times. This shows that for the 2008 storm, there would have been peak reductions in the majority of the subwatershed (at least there would not be peak increases) if the land cover would have been the one present pre-settlement. When analyzing the subwatersheds that presented the largest peak reduction (discharge simulated for 2001 was 2.8 times the discharge simulated for GLO) and the smallest peak reduction (discharge simulated for 2001 was 1.01 times the discharge simulated for GLO), it is possible to observe that the land cover transformation was more extreme for the subwatershed with the largest peak reduction (Figures 38 and 39). The CN for the watershed with the smallest peak reduction changed from 57.6 during the GLO to 68.8 during 2001 (difference in CNs of 11.2). On the other hand, the CN for the watershed with the largest peak reduction changed from 59.5 during the GLO to 73.4 during 2001 (difference in CNs of 13.9). This suggests that the land cover transformation had a role in the peaks observed when using the storm of 2008 as the rainfall input.

However, as discussed previously, flood events are caused by many factors besides the land cover, being the distribution and intensity of the rainfall an important factor. Therefore, the results of this thesis are only applicable to the 2008 event. Also, since this is the first set of data used with this model, and there is no data to validate these results for the time of the GLO, it is important to take these results with caution, and keep in mind that the reductions in peak discharge might be the result of nonlinear effects of changing the Curve Number.

These results however are so surprising and interesting, that it would be worth it to invest more resources to research this topic and to continue developing this model to capture the role of land cover in flooding. The model could be used with another event for which there is land cover, rainfall and discharge information. An option could be modeling the 2004 event, since that event produced significantly different flooding at

Eldorado and Elkader (Figure 7 and Figure 8). Another option would be to use the model in other watersheds that have had a different land cover transformation.

Finally, it is important to acknowledge that even if the effects on flooding of the land cover transformation simulated in this project were reproduced across time and space and with different rainfall events, it is not practical or maybe desirable to restore the current land cover to the pre-settlement state. Therefore as a management tool, it would be useful to run simulations using land cover transformations that are feasible, and analyze the flood reduction probabilities that these land covers offer.

Figure 35. Comparison of hydrographs for the May of 2004 flood event at Elkader using different time steps

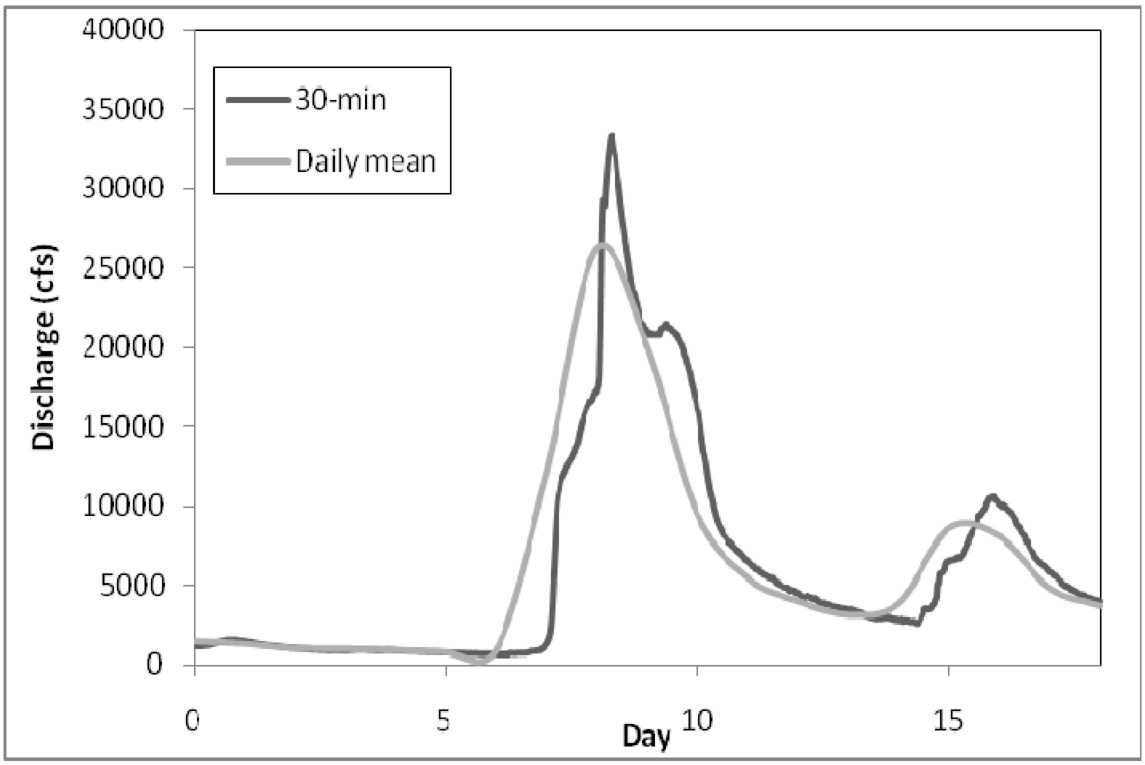

Figure 36. Rating Curve for the Turkey River at Elkader

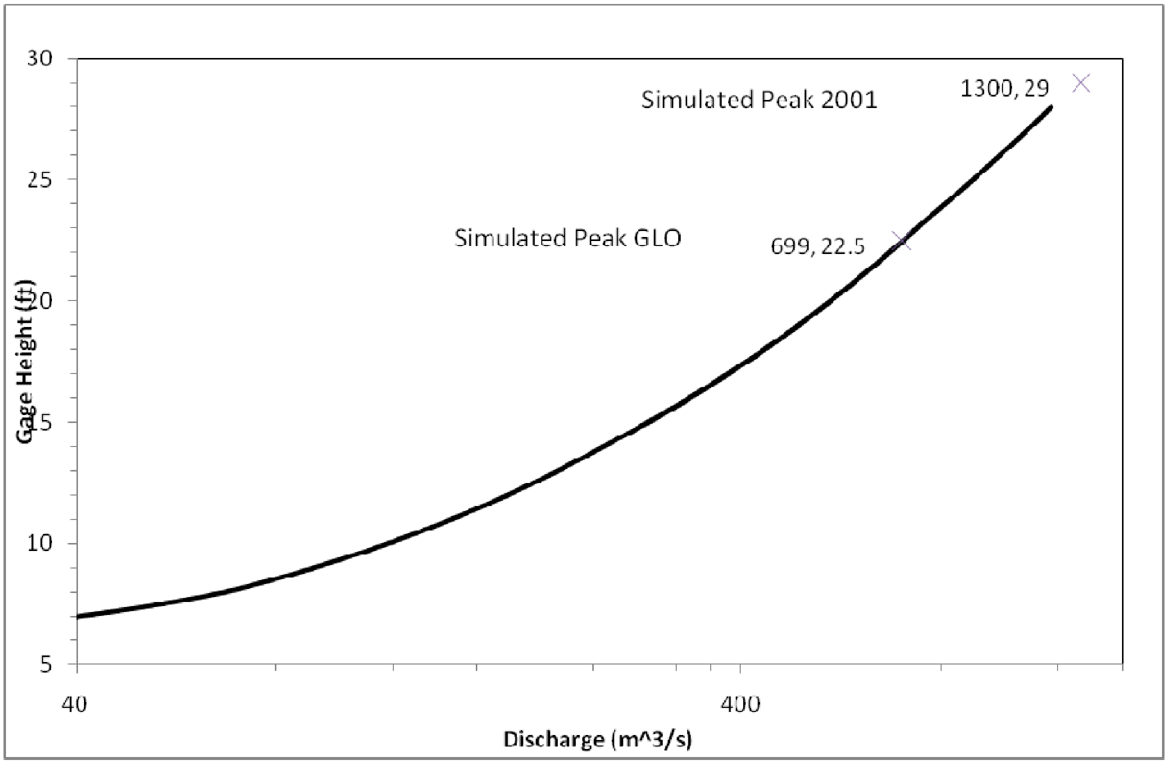

Figure 37. Relative peak flow reduction between using the 2001 and the GLO land covers

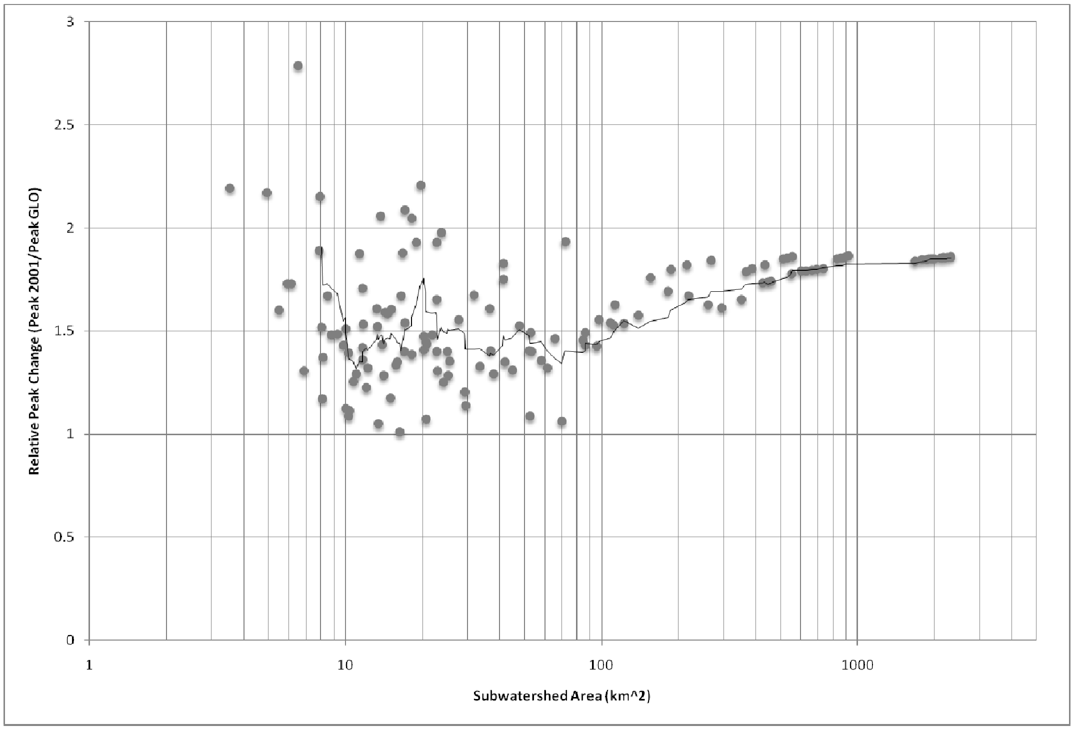

Figure 38. Location and land cover for subwatershed with the maximum simulated peak flow reduction (GLO discharge < 2001 Discharge)

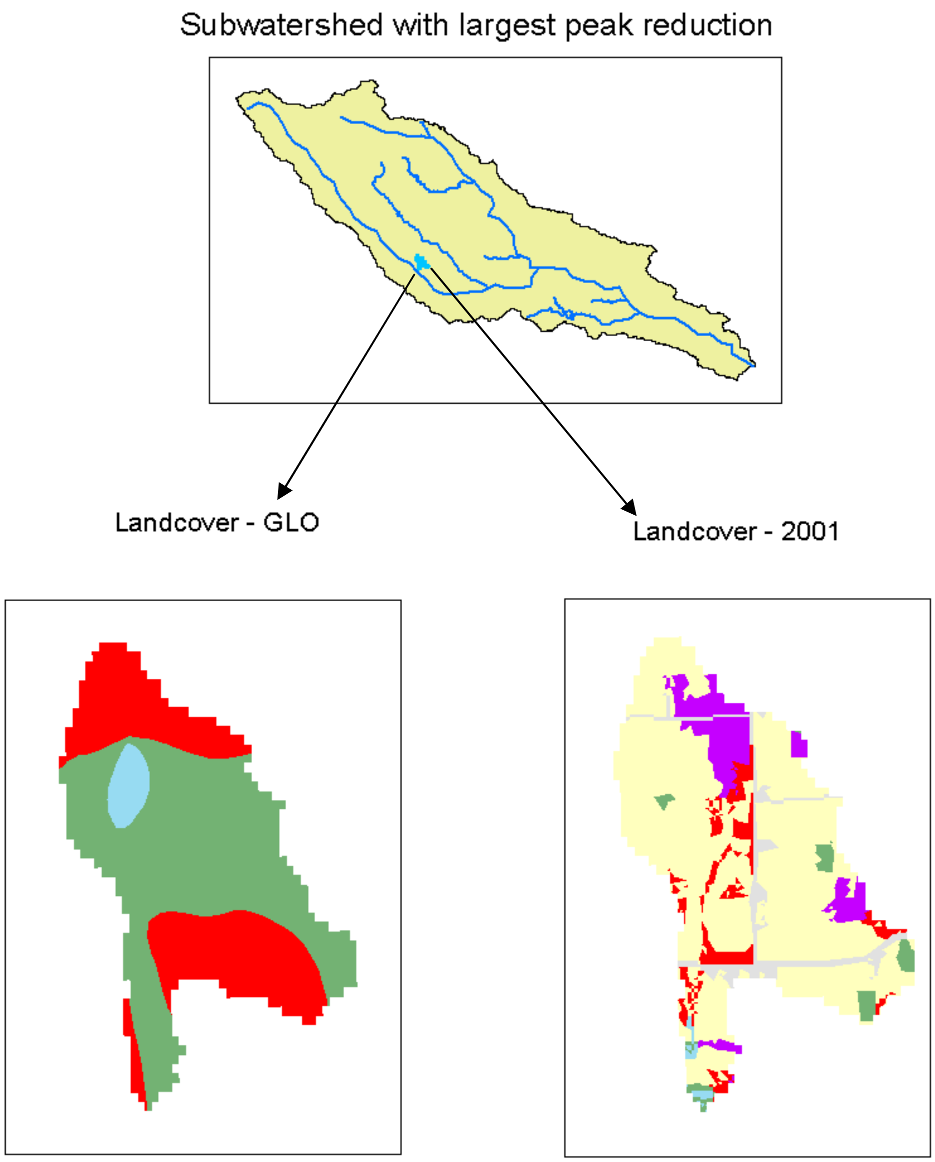

Figure 39. Location and land cover for subwatershed with the minimum simulated peak flow reduction (GLO discharge ≈2001 Discharge)

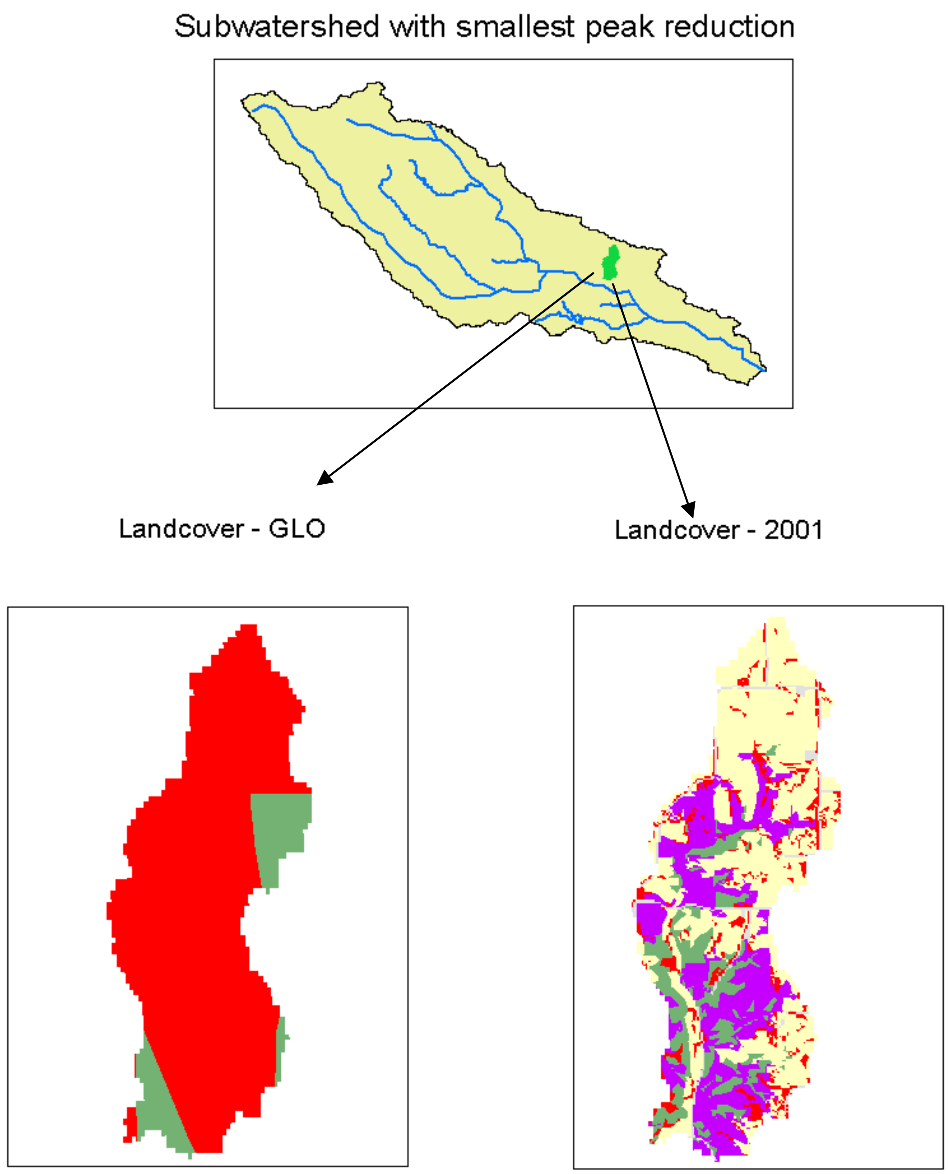

REFERENCES CITED

Andersen, O., T. R. Crow, S. M. Lietz, and F. Stearns. 1996. Transformation of a landscape in the upper mid-west, USA: The history of the lower st. croix river valley, 1830 to present. Landscape and Urban Planning **35**(4)**:**247-267.

Arnold, J. G., R. Srinivasan, R. S. Muttiah, and J. R. Williams. 1998. Large area hydrologic modeling and assessment part I: Model development. JAWRA Journal of the American Water Resources Association **34**(1)**:**73-89.

Asbjornsen, H., G. Mora, and M. J. Helmers. 2007. Variation in water uptake dynamics among contrasting agricultural and native plant communities in the midwestern U.S. Agriculture, Ecosystems & Environment **121**(4)**:**343-356.

Bharati, L., K. H. Lee, T. M. Isenhart, and R. C. Schultz. 2002. Soil-water infiltration under crops, pasture, and established riparian buffer in midwestern USA. Agroforestry Systems **56**(3)**:**249-257.

Blann, K. L., J. L. Anderson, G. R. Sands, and B. Vondracek. 2009. Effects of agricultural drainage on aquatic ecosystems: A review. Critical Reviews in Environmental Science and Technology **39**(11)**:**909.

Borah, D. K., and M. Bera. 2004. Watershed-scale hydrologic and nonpoint-source pollution models: Review of applications. Trans. ASAE **47**(3)**:**789-803.

Brye, K. R., J. M. Norman, L. G. Bundy, and S. T. Gower. 2000. Water-budget evaluation of prairie and maize ecosystems. Soil Science Society of America Journal **64**(2)**:**715-724.

Burkart, M. 2010. The Hydrologic Footprint of Annual Crops. Pages 77-86 in C. F. Mutel, editor. A Watershed Year: Anatomy of the Iowa Floods of 2008. University of Iowa Press, Iowa City, IA.

Canadell, J., R. B. Jackson, J. B. Ehleringer, H. A. Mooney, O. E. Sala, and E. D. Schulze. 1996. Maximum rooting depth of vegetation types at the global scale. Oecologia **108**(4)**:**583-595.

Changnon, S. A., and M. Demissie. 1996. Detection of changes in streamflow and floods resulting from climate fluctuations and land use-drainage changes. Climatic Change **32** (4):411-421.

Craine, J. M., D. A. Wedin, F. S. III Chapin, and P. B. Reich. 2003. Relationship between the structure of root systems and resource use for 11 north american grassland plants. Plant Ecology **165**(1)**:**85-100.

Cunha, L. K., W. F. Krajewski, and R. Mantilla. 2011. A framework for flood risk assessment under nonstationary conditions or in the absence of historical data. Journal of Flood Risk Management **4**(1)**:**3-22.

Downer, C. W., F.L. Ogden, J. Neidzialek, and S. Liu. 2006. Gridded Surface/Subsurface Hydrologic Analysis (GSSHA) Model: A Model for Simulating Diverse Streamflow-Producing Process. Pages 131-157 in V. P. Singh and D. K. Frevert, editors. CRC Taylor and Francis, Boca Raton, Fla.

Federal Emergency Management Agency (FEMA). 2011. FEMA Map Service Center. . Available from http://www.msc.fema.gov (accessed on May 30th, 2011).

Feldman, A. 2000. Hydrologic Modeling System-HEC-HMS-Technical Reference Manual. US Army Corps of Engineers, Davis, CA.

Fitzpatrick, F. A., J. C. Knox, and H. E. Whitman. 1999. Effects of Historical Land-Cover Changes on Flooding and Sedimentation, North Fish Creek, Wisconsin. United States Geological Service Water Resources Investigations Report 99-4083. 12 p.

Graham, D. N., and M. Butts. 2006. Flexible, integrated watershed modelling with MIKE SHE. Pages 245-272 in V. P. Singh and D. K. Frevert, editors. Watershed Models. CRC Taylor and Francis, Boca Raton, Fla.

Gupta, V., and E. Waymire. 1998. Spatial variability and scale invariance in hydrologic regionalization. Pages 88–135 in G. Sposito, editor. Scale Dependence and Scale Invariance in Hydrology. Cambridge University Press, Cambridge, UK.

Guttman, N. B., J. R. M. Hosking, and J. Wallins. 1994. The 1993 midwest extreme precipitation in historical and probabilistic perspective. Bulletin of the American Meteorological Society **75**(10)**:**1785-1792.

Hejazi, M. I., and M. Markus. 2009. Impacts of urbanization and climate variability on floods in northeastern Illinois. Journal of Hydrologic Engineering **14**(6)**:**606-616.

Huff, Floyd A., and J. R. Angel. 1992. Rainfall Frequency Atlas of the Midwest. Illinois State Water Survey, Champaign, Bulletin 71. 141 p.

Iowa Department of Natural Resources (IA DNR). 2011. Natural Resources Geographic Information Systems Library. Available from http://www.igsb.uiowa.edu/nrgislibx/ (accessed on May 30th, 2010).

Iowa Flood Center (IFC). 2011. Iowa Floods Information System (IFIS). Available from http://ut.iihr.uiowa.edu/ifis/ (accessed on May 31st, 2011).

Jackson, L., and D. Keeney. 2010. Perennial Farming Systems that Resist Flooding. Pages 215-225 in C. F. Mutel, editor. A Watershed Year: Anatomy of the Iowa Floods of 2008. University of Iowa Press, Iowa City, IA.

Jackson, B. M., H. S. Wheater, N. R. Mcintyre, J. Chell, O. J. Francis, Z. Frogbrook, M. Marshall, B. Reynolds, and I. Solloway. 2008. The impact of upland land management on flooding: Insights from a multiscale experimental and modelling programme. Journal of Flood Risk Management **1**(2)**:**71-80.

Kokkonen, T. 2003. Rainfall-runoff modelling – comparison of modelling strategies with a focus on ungauged predictions and model integration. Doctor of Philosophy dissertation. Helsinki University of Technology, Water Resources Publications, Espoo.

Krajewski, W. F., and R. Mantilla. 2010. Why Were the 2008 Floods So Large? Pages 19-30 in C. F. Mutel, editor. A Watershed Year: Anatomy of the Iowa Floods of 2008. University of Iowa Press, Iowa City, IA.

Love, O. 2010. Serious thought given to whether ag tiling helps or harms. Available from http://thegazette.com/2010/07/18/serious-thought-given-to-whether-ag-tiling-helps-or-harms/ (accessed on May 30, 2010).

Mantilla, R. 2007. Physical Basis of Statistical Scaling in Peak Flows and Stream Flow Hydrographs for Topologic and Spatially Embedded Random Self-similar Channel Networks. Doctor of Philosophy dissertation. Department of Civil and Environmental Engineering, University of Colorado, Boulder, Colorado.

Mantilla, R. 2011. Nonlinear velocity parameters for the Turkey River Basin. Personal Communication.

Mantilla, R., and V. K. Gupta. 2005. A GIS numerical framework to study the process basis of scaling statistics in river networks. IEEE Geoscience and Remote Sensing Letters **2**(4)**:**404-408.

Mantilla, R., V. K. Gupta, and O. J. Mesa. 2006. Role of coupled flow dynamics and real network structures on hortonian scaling of peak flows. Journal of Hydrology **322**(1-4)**:**155-167.

McIntyre, N., and M. Marshall. 2010. Identification of rural land management signals in runoff response. Hydrological Processes **:**.

Mishra, S. K., and V. P. Singh. 2003. Soil Conservation Service Curve Number (SCS-CN) Methodology. Kluwer Academic Publishers, Dordrecht, The Netherlands.

Mitsch, W. J., and J. G. Gosselink. 2007. Wetlands. John Wiley & Sons, Hoboken, N.J.

Natural Resources Conservation Service (NRCS). 2011. Soil Survey Geographic (SSURGO) Database. Available from http://soildatamart.nrcs.usda.gov/ (accessed on May 30th, 2010).

NOAA Satellite and Information Center. 2008. 2008 Midwestern Floods. Available from http://www.ncdc.noaa.gov/special-reports/2008-floods.html (accessed on May 30th, 2010).

O'Callaghan, J. F., and D. M. Mark. 1984. The extraction of drainage networks from digital elevation data. Computer Vision, Graphics, & Image Processing **28**(3)**:**323-344.

Ponce, V. M., and R. H. Hawkins. 1996. Runoff curve number: Has it reached maturity? Journal of Hydrologic Engineering **1**(1)**:**11-19.

Prior, J. C. 1991. Landforms of Iowa. Department of Natural Resources, University of Iowa Press, Iowa City, Iowa.154 p.

Reungsang, P., R.S. Kanwar, M. Jha, P.W. Gassman, K. Ahmad, and A. Saleh. 2005. Calibration and validation of SWAT for the Upper Maquoketa River watershed. Center for Agricultural and Rural Development. Iowa State University. Working Paper 05-WP-396. 19 p.

Schilling, K. E. 2005. Relation of baseflow to row crop intensity in iowa. Agriculture, Ecosystems & Environment **105**(1-2)**:**433-438.

Schilling, K. E., and M. Helmers. 2008. Tile drainage as karst: Conduit flow and diffuse flow in a tile-drained watershed. Journal of Hydrology **349**(3-4)**:**291-301.

Schilling, K. E., and R. D. Libra. 2003. Increased baseflow in iowa over the second half of the 20th century. Journal of the American Water Resources Association **39**(4)**:**851-860.

Singh, V. P., and D. K. Frevert, editors. 2006. Watershed Models. CRC Taylor and Francis, Boca Raton, Fla.

Sivakumar, B. 2008. Dominant processes concept, model simplification and classification framework in catchment hydrology. Stochastic Environmental Research and Risk Assessment **22**(6): 737-748.

Skaggs, R. W., M. A. Breve, and J. W. Gillian. 1994. Hydrologic and water quality impacts of agricultural drainage. Critical Reviews in Environmental Science and Technology **24**(1)**:**1-32.

Smedema, L. K., W. F. Vlotman, and D. W. Rycroft. 2004. Modern Land Drainage. Planning, Design and Management of Agricultural Drainage Systems. A.A. Balkema Publishers, Leiden, The Netherlands.

Tufekcioglu, A., J. Raich, T. Isenhart, and R. Schultz. 1998. Fine root dynamics, coarse root biomass, root distribution, and soil respiration in a multispecies riparian buffer in central iowa, USA. Agroforestry Systems **44**(2)**:**163-174.

U.S. Census Bureau. 2009. The 2009 Statistical Abstract. Available from http://www.census.gov/compendia/statab/cats/geography_environment/land_and_land_use.html (accessed on April 13th, 2010).

United States Department of Agriculture (USDA). 2011. National Agricultural Statistics Service. Available from http://www.nass.usda.gov/ (accessed on May 30th, 2010).

United States Geological Service (USGS). 2010a. Instantaneous Data Archive. Available from http://ida.water.usgs.gov/ida/index.cfm (accessed on May 30th, 2010).

United States Geological Service (USGS). 2010b. Seamless data warehouse. Available from http://seamless.usgs.gov/ (accessed on May 30th, 2010).

United States Geological Service (USGS). 2011a. National Water Information System. Available from http://water.usgs.gov/data/ (accessed on May 30th, 2011).

United States Geological Service (USGS). 2011b. Streamflow Measurements for Iowa. Available from http://waterdata.usgs.gov/ia/nwis/measurements/?site_no=05412020 (accessed on May 30th, 2010).

United States Geological Service (USGS). 2011c. Water Data Report 2008 - 05412020 Turkey River Above French Hollow Creek at Elkader, IA. Available from http://wdr.water.usgs.gov/wy2008/pdfs/05412020.2008.pdf (accessed on May 30th, 2010).

Wehmeyer, L. L., F. H. Weirich, and T. F. Cuffney. 2011. Effect of land cover change on runoff curve number estimation in iowa, 1832-2001. Ecohydrology **4**(2)**:**315-321.

Young, P. C. 2002. Data-based mechanistic and top-down modeling. Pages 363-374 in A. E. Rizzoli and A. J. Jakeman, editors. IEMSs 2002. International Environmental Modelling and Software Society, Lugano, Switzerland.

Zhang, L., W. R. Dawes, and G. R. Walker. 2001. Response of mean annual evapotranspiration to vegetation changes at catchment scale. Water Resources Research **37**(3)**:**701-708.

Zhang, Y. K., and K. E. Schilling. 2006. Effects of land cover on water table, soil moisture, evapotranspiration, and groundwater recharge: A field observation and analysis. Journal of Hydrology **319**(1-4)**:**328-338.

Zingula, C. 2010. Agricultural tile helps manage watershed. Available from http://thegazette.com/2010/05/02/agricultural-tile-helps-manage-watershed/ (accessed on May 30, 2010).